NATIONAL URANIUM TAILINGS PROGRAM

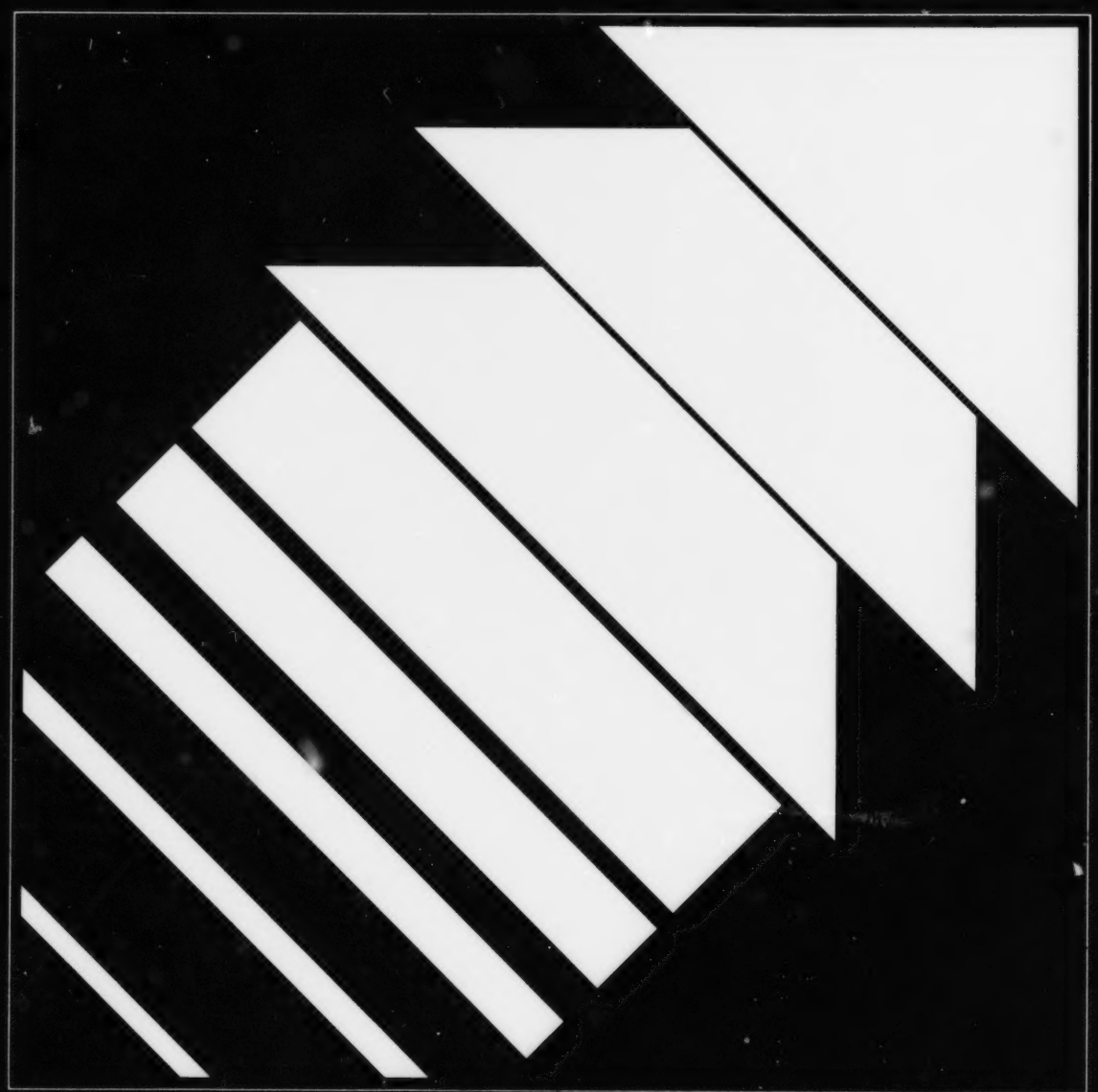

Energy, Mines and Resources Canada | Énergie, Mines et Ressources Canada

Canada

STUDY OF RADIUM-226 CO-PRECIPITATES IN URANIUM MILL TAILINGS BY SECONDARY ION MASS SPECTROMETRY

DSS FILE #15SQ.23241-5-1718

CONTRACT REPORT NUMBER OSQ85-00289
CONTRACTOR Atlantic Nuclear Services Ltd.
DSS REQUISITION NUMBER 15SQ23241-5-1718

A Research Report Prepared for

The National Uranium Tailings Program

Canada Centre for Mineral and Energy Technology
Energy Mines and Resources Canada
555 Booth Street
Ottawa, Ontario
K1A 0G1

by

Atlantic Nuclear Services Ltd.
P. O. Box 1268, Station A
Fredericton, N. B.
E3B 5C8

James J. McGrath, P.Eng.
Project Manager

Stephen Chryssoulis, Ph.D.
Principal Investigator
New Brunswick Research and Productivity Council
College Hill Road, Fredericton, N. B.

Co-Investigators

K. D. Burns, Atomic Energy of Canada Ltd.
Darlene Johnston, Surface Science Western
Stuart N. McIntyre, Surface Science Western

July 23, 1986

66pp

MICROMEDIA

TABLE OF CONTENTS

		Page
1.0	ABSTRACT	1
2.0	RECOMMENDATIONS	2
3.0	INTRODUCTION	4
4.0	SAMPLE PREPARATION	6
5.0	RESULTS	10
5.1	Mineralogical Analysis	10
	5.1.1 Barium Mineralogy	10
	5.1.2 Lead Mineralogy	14
	5.1.3 Primary and Secondary Barium and Lead Sulphate	18
5.2	The Ion Microprobe	18
	5.2.1 Description	18
	5.2.2 Operating Conditions	20
	5.2.3 Standardization	22
	5.2.4 Preparation of Standards	24
	5.2.5 Development of the Technique	26
	5.2.6 Calibration of the Ion Microprobe	27
5.3	Determination of the Radium Concentration in the Elliot Lake Barite	34
6.0	DISCUSSION	36
6.1	Occurrence of Barium in Pachuca Solids	36
6.2	Occurrence of Lead in Pachuca Solids	36
6.3	Proposed Mechanism for the Dissolution and Precipitation of Radium, Barium and Lead in the Leach Process	37
6.4	Determination of Radium in Barium and Lead Sulphate by SIMS	39
7.0	CONCLUSIONS	43
8.0	ACKNOWLEDGEMENTS	45
	LIST OF REFERENCES	46
	APPENDIX A1	
	A2 (under separate cover)	
	A3	
	A4	

1.0 ABSTRACT

In-situ determination of the distribution of ^{226}Ra between barium and lead sulphate co-precipitates from uranium ore leaching was undertaken using Secondary Ion Mass Spectrometry (SIMS) under contract to the National Uranium Mine Tailings Program.

Development of the method including definition of the limits of detectability and grain size were established.

Mineralogical examination of leached solids revealed the presence of primary Barium and Lead Sulphates. Barium Sulphates contained very low concentrations of Radium upon analysis by SIMS technique. Barium-rich feldspars were identified.

Secondary co-precipitates were not analyzed due to loss of smaller particles during sample preparation and incomplete understanding of ore mineralogy at the time.

2.0 RECOMMENDATIONS

A credible predictive model for the release of radium into the environment requires in addition to the identification, the quantitative determination of the radium between the various forms in which it is present in the uranium tailings. Because of the rapidly changing conditions during the uranium ore treatment, non equilibrium or local equilibrium conditions may prevail, resulting in the presence of radium in more than one form in the tailings. The stability of the different forms varies considerably, the most stable being radium co-precipitated with barium sulphate and the most unstable being radium adsorbed on the surface of mineral grains.

Sensitive analytical tools are now available for the in-situ determination of (i) radium in solid solution in barium and lead sulphate (Secondary Ion Mass Spectrometry, SIMS), or (ii) radium adsorbed on the surface of mineral grains (X-ray Photoelectron Spectroscopy, XPS; and Scanning Auger Microscopy SAM). The SIMS detection limit for radium is in the ppb range. Areas as small as 100 μm^2 were analyzed. XPS enables the semiquantitative analysis of all elements (except H and He) present in a surface layer 1-2 nm thick with detection limits of 0.02-0.2% a/a corresponding to 1-10% of a monolayer. The area of analysis has a diameter of 150 µm. SAM has a much higher spacial resolution (50 nm) than XPS, but the detection limits are one order of magnitude better.

The following determinations will enable the identification and quantification of the various forms in which radium is present in the uranium tailings thus providing the experimental data necessary for modelling the radium release to the environment:

-Determination of the radium content of secondary barite ($BaSO_4$) and anglesite ($PbSO_4$), including the anglesite coating of galena particles by the most recently developed SIMS technique (IMS-4F). Determination of the radium distribution between secondary barite

and anglesite. Quantification of primary and secondary barite. Special sample preparation is required in order to preserve and preconcentrate the sulphate precipitates.

-Identification of the presence of radium adsorbed on the surface of potassium feldspar crystals by XPS or SAM. Calibration by immersion of feldspar crystals in radium solution. Quantification of the adsorbed radium by balancing the radium in the solids and the solution prior to final neutralization. The sample preparation involves sieving of a sample of the final tailings. Although the amount of radium adsorbed is expected to be small, this radium is readily leachable under acidic conditions and therefore it is the first to be released to the environment.

3.0 INTRODUCTION

The objective of this study was to develop an in-situ micro-analytical technique for the quantitative determination of radium, present at low-part-per-million concentration levels in barium and lead sulphate grains (Appendix A1). Previous studies have shown that most of the radium released during the leaching of uranium ore with sulphuric acid is co-precipitated with either barium or lead sulphate and consequently reports to the tailings. The re-dissolution of radium in the tailings and subsequent release into the environment depends on the solubility properties of the host precipitate.

The identification of the physical state of radium after uranium ore leaching is pivotal in understanding the geochemical mechanisms controlling its dissolution in uranium tailing sites. Most of the available evidence on the state of radium is based on leaching studies of radium containing tailings or intermediate products of uranium leaching plants, by a variety of aqueous media of different acidity, salt content and complexing reagents. Selective dissolution properties of the medium on lead and barium sulphate are employed. However, several factors including the presence of barium or lead sulphate of more than one origin having different radium content, abundance, range of grain size and solubility rate may complicate the situation and lead to inconclusive results. It has been also reported that radium will adsorb readily on phyllosilicate minerals (Beard et al., 1979) especially during neutralization of the tailings.

The quantitative determination of radium in uranium tailings by employing in-situ microanalytical techniques will enable the direct identification of the phases in which radium is present. Thus its release in the long term can be modelled on the basis of the dissolution behaviour of the host material.

The expected concentration of radium in the barium and lead sulphate is in the low ppm and possibly ppb range, which is below the detection limit of the electron microprobe (200-500 ppm). In-situ microanalytical techniques more sensitive than electron probe microanalysis are now available. They include Particle Induced X-ray Emission (PIXE), Laser Induced Mass Analysis (LIMA) and Secondary Ion Mass Spectrometry (SIMS). SIMS was selected for the radium determinations because it is better characterized and more sensitive than the other methods. Recently, silver concentrations of a few ppm were analyzed with accuracy and precision better than 15% (Chryssoulis et al., 1986).

The developed SIMS method was used to determine the radium content of barium and lead sulphate crystals identified in a solid sample from the Pachuca leach of Rio Algom.

4.0 SAMPLE PREPARATION

A solid sample was obtained from Rio Algom Ltd. in Elliot Lake, Ontario, from the Pachuca leach before neutralization with lime. This minimized the amount of gypsum in the sample to avoid relatively high concentrations of sulphate which can affect the dissolution of barium and lead sulphates. The sample was split into two fractions. One fraction was sent to Chemex Laboratories Ltd. to investigate the repetitive batch water extraction of barium, lead and radium from the radium bearing leached ore. Steger and LeGeyt (1986) discuss the results of this study. The other fraction was dried and sent to the Research and Productivity Council (RPC) for SIMS analysis. The chemical composition of a dried portion of the sample is given in Table 1.

In order to preconcentrate the barium and lead sulphate for the SIMS analysis, the sample was initially screened into the following size fractions: +100 mesh, -100+150 mesh, -150+325 mesh and -325 mesh. A portion of each sized fraction was separated gravimetrically using heavy liquid media (2.90 $g.cm^{-3}$) into a heavy and a light fraction. Further, a portion of the -100+150 mesh heavy fraction was separated with a Frantz isodynamic separator into a magnetic and a non-magnetic fraction.

The various fractions were analyzed by Bondar-Clegg for barium and lead by atomic absorption (Table 2). The concentration of barium and lead increased with decreasing grain size and in the same size fraction was higher in the heavy fraction. Most of the barium in the heavy fraction should be in the form of barium sulphate (barite), however it was below the detection limit of the XRD (2,500 ppm).

In the light fraction barium is probably in the potassium feldspar. Lead sulphide (galena) and lead sulphate (anglesite) account for most of the lead in the heavy fraction while in the

Table 1. Chemical Composition of Leached Ore Sample*

	Mass wt%		µg/g
Fe	2.67	Ra	710
Al	3.20	Pb	345
K	2.24		
Ti	0.20	Ra-226	7.25 Bq/g
Na	0.18		
Mg	0.09		
Ca	0.10		

* Dried weight basis

Original moisture content was 10.7%

"Exchangeable" or "Easily Extractable" Ra-226 = 3.88 Bq/g

(from Steger and LeGeyt, 1986)

Table 2. Concentration of barium and lead in sized and gravity fractions

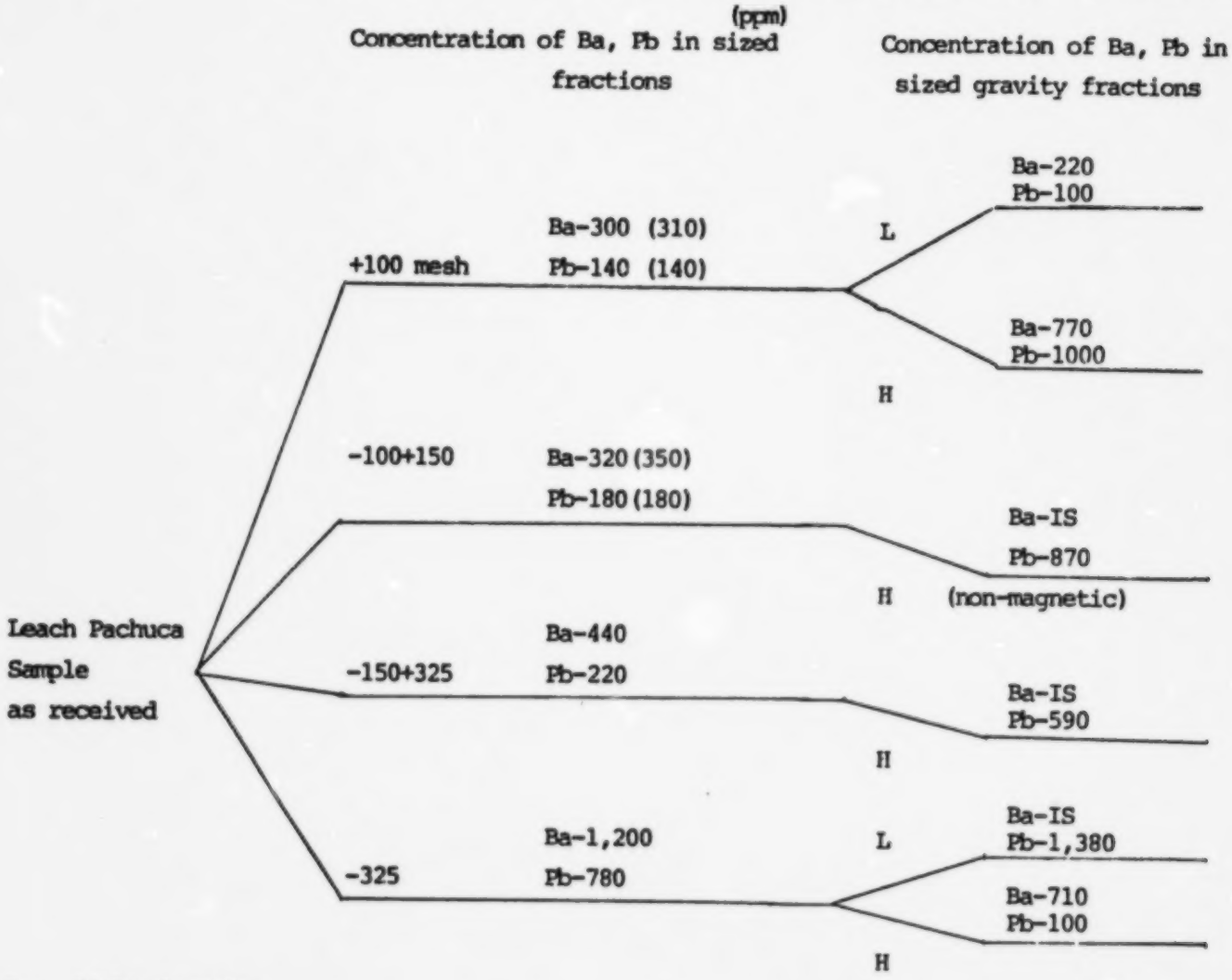

L: light fraction
H: heavy fraction
IS: insufficient sample

light fraction a significant amount of lead could be present in the potassium feldspar.

Polished blocks and thin sections of the heavy fractions and the finest light fraction were prepared. As the use of the ion microprobe requires for practical purposes, the pre-identification of the grains to be analyzed, barium and lead sulphate grains were found with the optical and the scanning electron microscope. Their composition was verified with the energy dispersive analyzer and their homogeneity checked by viewing their backscattered back-scattered electron (BSE) image. A photograph of the BSE image was taken to facilitate the location and the identification of the grains to be analyzed with the ion microprobe (Appendix A2).

5.0 RESULTS

The results of the mineralogical examination required for the ion microprobe analysis are reported first. The development of the SIMS technique and the calibration of the ion microprobe for the determination of radium in barium and lead sulphate are discussed in the second part of this section while the ion microprobe results on the radium content of the Elliot Lake barium and lead sulphate are reported last.

5.1 Mineralogical Analysis

Pyrite is the main component of the heavy fractions. Quartz, K-feldspar, sericite, rutile, monazite, iron oxides, barite, iron-free and iron bearing sphalerite, chalcopyrite, stibnite and galena are present in minor amounts. Small (less than 2 µm) brannerite inclusions in pyrite and uraninite and thorianite inclusions in monazite were identified (Figure 1). Quartz and K-feldspar predominate in the light fraction. Sericite and unliberated pyrite and monazite are also present.

5.1.1 Barium Mineralogy

Barium is present in the form of barite ($BaSO_4$) which in the +100 mesh size, is further concentrated in the heavy fraction. Barite particles were identified in all size fractions. It is always free with a few exceptions, where it is associated with quartz (Figure 2). In total more than fifty grains of barite ranging in size from ten to one hundred microns were identified with the SEM. Back-scattered images of these primary barite grains are presented as Appendix A2 under separate cover. The grain size and fragmented nature of the barite grains is indicative of their primary origin. Barite from the ore is classified as primary barium sulphate as opposed to any barium sulphate crystals which precipitate during the ore processing (secondary barium sulphates). All barite grains were fragments with the

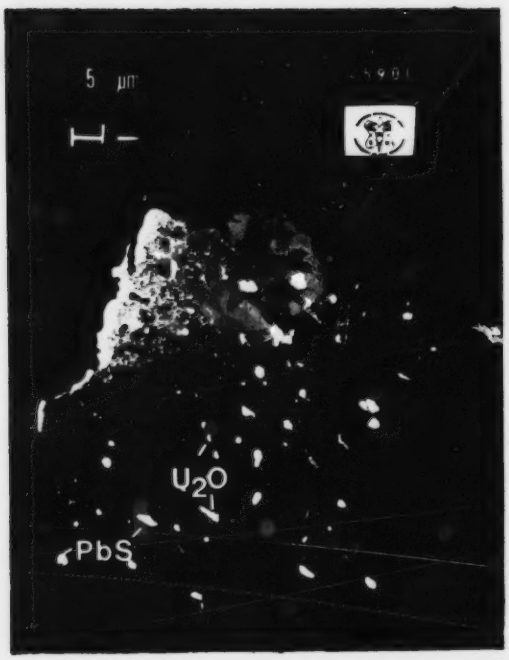

FIGURE 1. Uraninite (UO_2) and galena (PbS) inclusions in monazite.

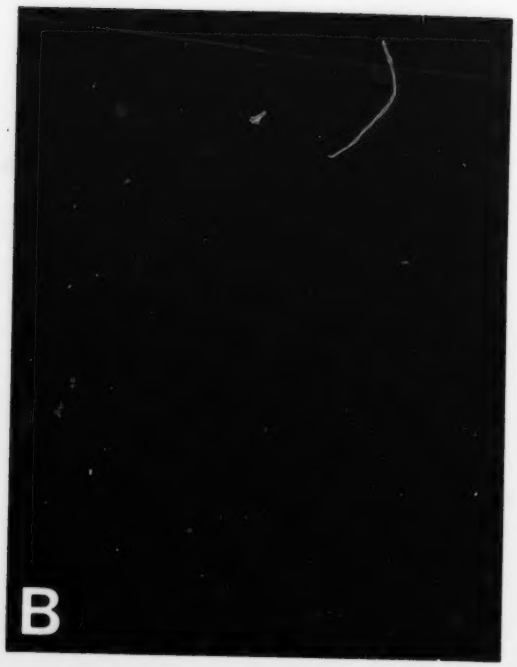

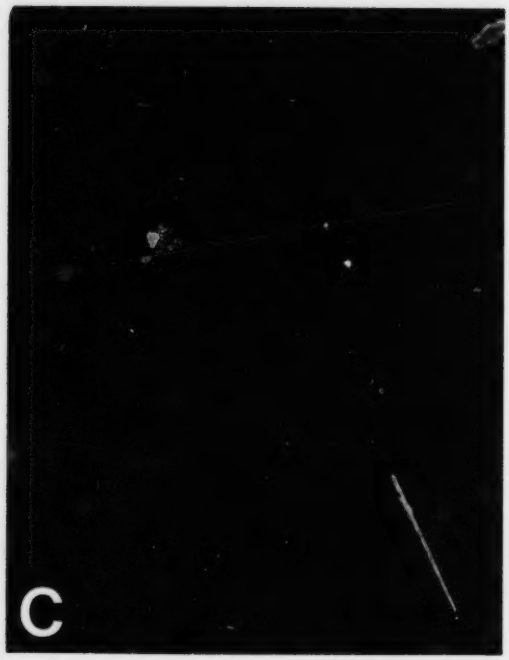

FIGURE 2: Barite interlocked with quartz. A. backscattered electron image. B: ion image of $^{28}Si^{+}$. C. ion image of $^{138}Ba^{+}$.

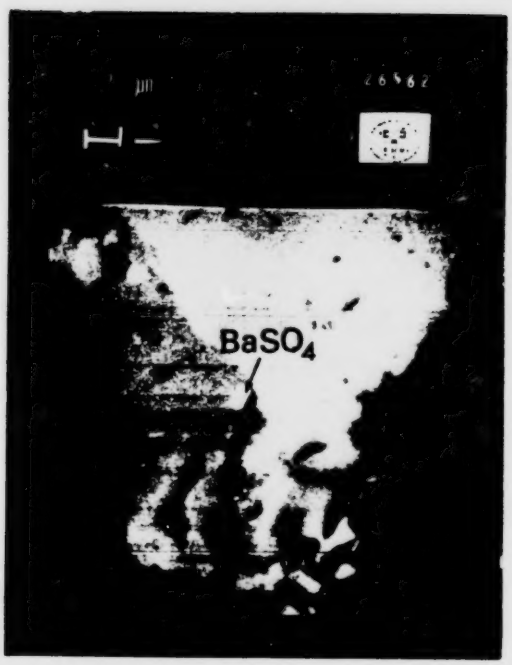

FIGURE 3. Barite in seritized potassium feldspar.

exception of one euhedral 2 μm barite crystal identified along the contact of sericite with a K-feldspar crystal (Figure 3). The potassium feldspar contained barium which presumably formed barite during sericitization.

The concentration of barium in solid solution in the potassium feldspars ranges from below the detection limit of the electron microprobe in the energy dispersive mode (~0.3 wt%) up to 6 wt% (Table 3). An enrichment in barium in the latter stages of the potassium feldspar crystallization is evident from the BSE images (Figure 4). The rims and fractures of Ba-bearing potassium feldspars were closely examined for barium sulphate crystals (secondary barite) with magnifications of X10,000 and X20,000 (detection limits 0.1 and 0.05 μm respectively). None were detected.

Energy conservation considerations, the common ion effect and the excess of sulphate ions in the Pachuca leach dictate that secondary barium sulphate should precipitate preferentially, on hydrolyzing Ba-bearing potassium feldspar and on primary barite crystals. However the nucleation of 'free' secondary barium sulphate is not excluded. Precipitation experiments of synthetic barite (Section 5.4) in the laboratory indicated that the expected range of grain size should be approximately 10 μm. The failure to identify secondary barium sulphate in this study is attributed to detachment and dissolution during the sample preparation.

5.1.2 Lead Mineralogy

In the ore, lead is present mainly in the form of galena (lead sulphide), free or enclosed in pyrite. Potassium feldspars may also account for some of the lead, however analyses for lead in the Elliot Lake potassium feldspars are not available. A few 1 μm galena inclusions were identified in the potassium feldspar crystals but not on the surfaces when examined at high magnifications for lead compounds. A large anglesite (or cerussite) crystal was found, originating probably from the ore.

Table 3. Barium Content of Barium-rich Potassium Feldspar

Grain	Ba (wt%)
1.	0.33
2.	0.96
3.	0.34
4.	6.07
5.	4.82
6.	3.75
7.	<0.30
8.	1.47

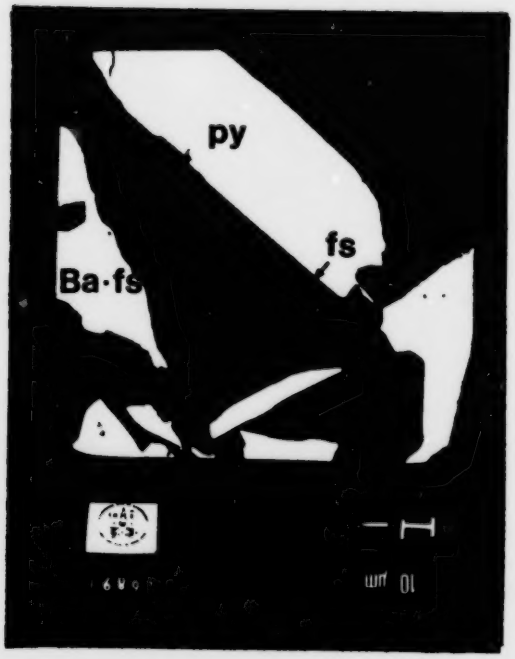

FIGURE 4. BSE image of potassium feldspar (grey) combined with pyrite (py: white). The light grey area is enriched in Barium. The barium is in solid solution in the feldspar with Ba++ replacing K+. Note the inhomogeneous distribution of barium-rich feldspar grain (Ba.fs). The dark zone between the Ba-rich feldspar and the pyrite is Ba-poor feldspar (fs).

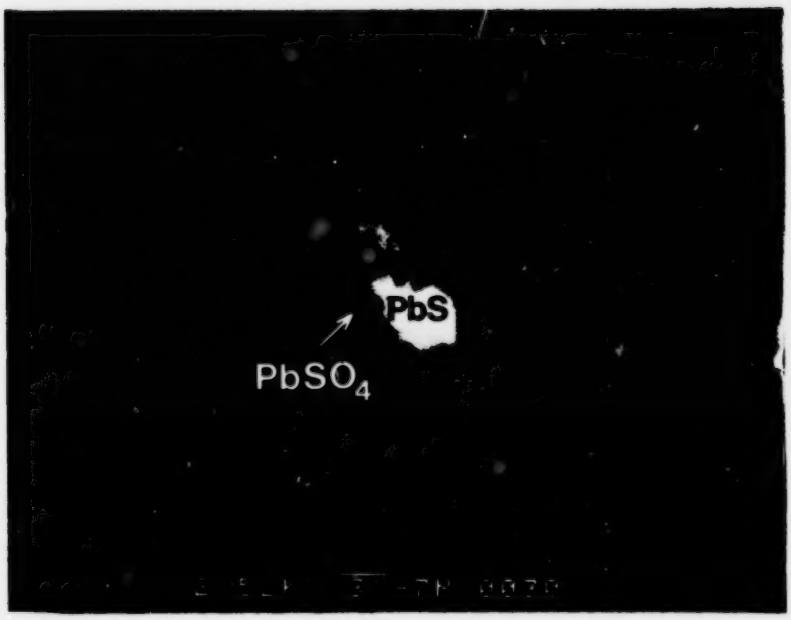

FIGURE 5: Oxidized galena grain

Most of the free galena grains in the sample, especially the smaller ones, have an oxidation coating (Figure 5). The thickness of the coating ranges from a small fraction of the average diameter of the galena grain to more than half the diameter in smaller grains. This coating formed during the Pachuca leach by the in-situ oxidation of the lead sulphide. Although the coating was not analyzed quantitatively it must be lead sulphate because of the excess of sulphate ions in the process. In addition, during the processing of the ore some lead will be released from the dissolving lead-bearing minerals which will precipitate as lead sulphate because of the excess of sulphate ions in the process. Therefore, from a genetic point of view two lead sulphate salts may be recognized: (i) lead sulphate forming in-situ by progressive in-ward oxidation of lead sulphide crystals and, (ii) lead sulphate precipitating from the solution in the Pachuca leach. The latter could be either 'free' or precipitated on favourable mineral surfaces.

5.1.3 Primary and Secondary Barium and Lead Sulphate

Sulphate minerals introduced into the process as such are identified as primary, as opposed to sulphate salts which form during the Pachuca leach which are classified as secondary. Criteria for their recognition include: grain size and shape, association with other minerals like quartz, and texture. This classification is important because secondary sulphate salts precipitating from the radium-bearing Pachuca leach solution will be enriched in radium relative to primary sulphate minerals. Under saturation conditions (for $PbSO_4$) the lead sulphate coating of lead sulphide grains may have an outer radium-enriched layer.

5.2 Ion Microprobe Measurements

5.2.1 Description

The instrument used in this study was a CAMECA IMS-3f ion microprobe (Figure 6). The primary ion beam is created in a cold

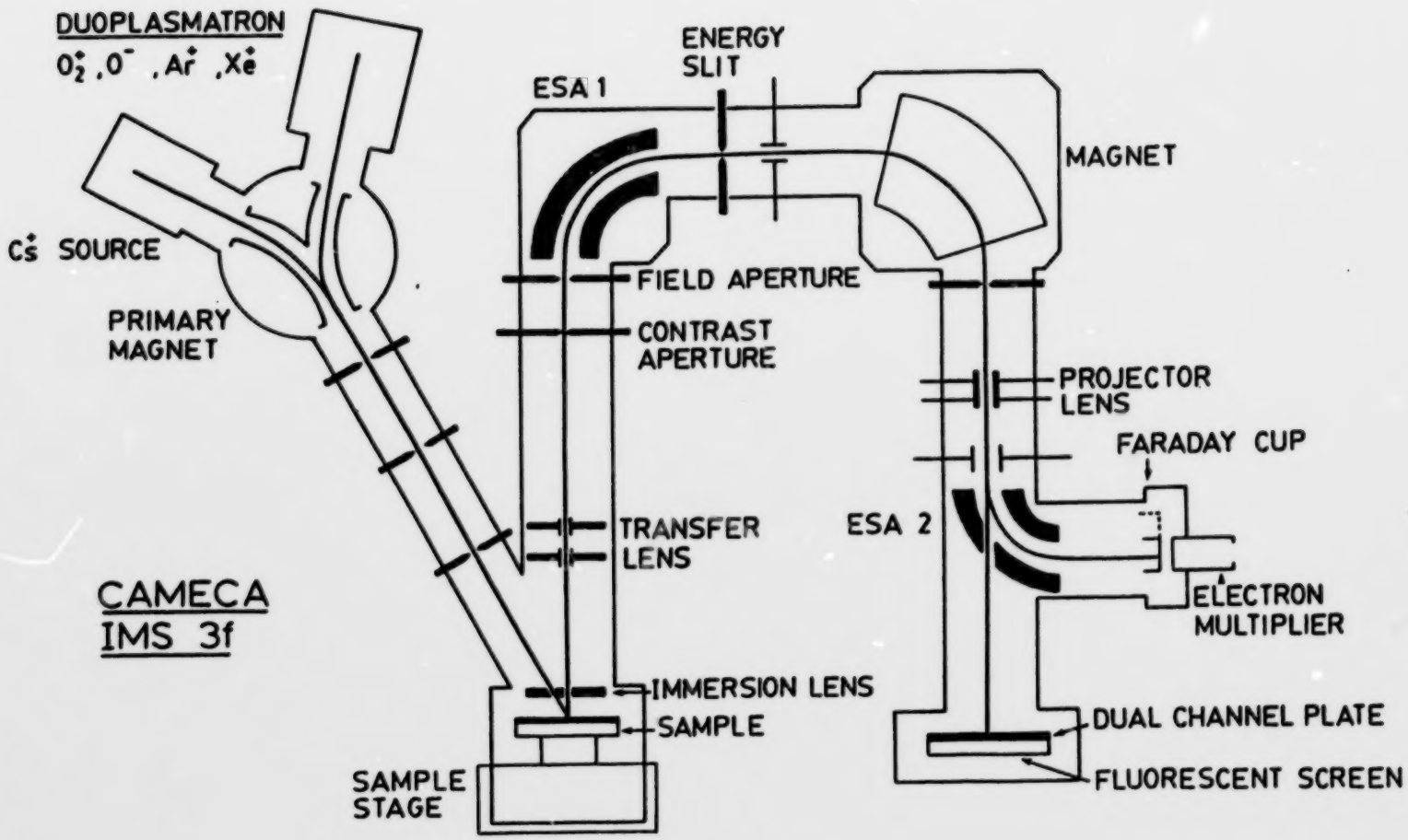

FIGURE 6: Schematic Diagram of the ion microprobe

cathode duoplasmatron or in a hot liquid metal source and then it is accelerated, mass filtered and focussed on the specimen surface. The beam can be focussed on a selected area. Several primary ion beams are available including O_2^+, O^-, N^+, Ar^+, Xe^+ and Cs^+.

The secondary ion beam is accelerated with the aid of an immersion lens at ground potential which is positioned at a distance of 0.5 mm from the surface of the specimen. A series of apertures in the primary column determine the size of the primary beam while apertures in the secondary column are adjusted to select the area of analysis and to eliminate secondary ions of low energy. The beam is directed to an electrostatic analyzer which discriminates between charged species on the basis of their energy and is then directed to the mass spectrometer. The secondary ion beam can be focussed onto a fluorescent screen for image display or directed to an electron multiplier for measurement.

5.2.2 Operating Conditions

Instrumental operating conditions are summarized in Table 4. An O^- beam was utilized because higher ion yields could be achieved for the elements of interest (Ra, Ba and Pb) without charging the carbon coated specimen. A preselected mineral grain was located using the optical microscope on the probe. The beam was rastered over an area of 150 by 150 μm or 100 by 100 μm, and the secondary ion image ($^{134}Ba^+$ for $BaSO_4$ or $^{206}Pb^+$ for $PbSO_4$) was examined to confirm that the beam was centered on the grain of interest. The beam was also used in the spot mode (60 μm). The area analyzed was a circle of 60 or 25 μm diameter in the centre of the rastered area as determined by a field aperture within the secondary optics. For the larger (primary) sulphate grains the analysis area was confined to a single grain. For smaller grains (less than 10 μm) only one grain was within the analysis area.

Table 4. Operating Conditions

Instrument	CAMECA IMS-3f Ion Microprobe
Primary Ions	O^-
Secondary Ions	$^{226}Ra^+$, $^{138}Ba^+$, $^{206}Pb^+$
Interfering Molecular Ions	$^{138}Ba^{88}Sr^+$ ($BaSO_4$)
	$^{208}Pb^{18}O^+$ ($PbSO_4$)
Primary Ion Energy	16.1 KeV
Primary Current	40-80 nA
Crater Size	60-150 μm square
Sampling Area	25-60 μm diameter circle
Mass Resolution	$M/\Delta M \sim 1{,}500$ ($BaSO_4$)
Kinetic Energy Offset	125-200V ($PbSO_4$)
Energy Slit	30eV

The $^{226}Ra^{+}$ isotope was monitored together with an isotope of the major cation in the sulphate matrix. A matrix isotope of relatively low abundance and free of molecular interferences was selected, $^{138}Ba^{+}$ for $BaSO_4$ and $^{206}Pb^{+}$ for $PbSO_4$. The intensity ratio of $^{226}Ra^{+}$ to the matrix isotope was used for determining the radium content of the sulphate by referring to a matrix-specific calibration curve, produced by analyzing synthetic barium or lead sulphate doped with known amounts of radium. Intensity ratios are less susceptible to matrix-induced or instrument related variations during the measurement (McIntyre et al., 1984).

5.2.3 Standardization

The use of the ion microprobe for in-situ trace elemental analysis has been limited by several factors inherent in the instrument and to the technique (Zinner, 1980). The secondary ion yields vary over four orders of magnitude from element to element (Figure 7) and are also strongly affected by the matrix (Chryssoulis, 1986). Additional difficulties arise because instrumental parameters and ion collection efficiencies vary from case to case (Leta and Morrison, 1980).

The use of closely matching standards is the most widely recognized method for obtaining quantitative measurements. Two methods for the production of closely matching standards are available. McIntyre et al., (1984) utilized synthetic minerals homogeneously doped with the trace element of interest, while Leta and Morrison (1980) employed a solid state standard addition method. Although the latter gives better sensitivity and is superior in accuracy and precision (Chryssoulis et al., 1986) it is not recommended for fine grained material. The present investigation used synthetic barium and lead sulphate doped with known amounts of radium. This technique reproduces the mineral matrix and gave satisfactory results.

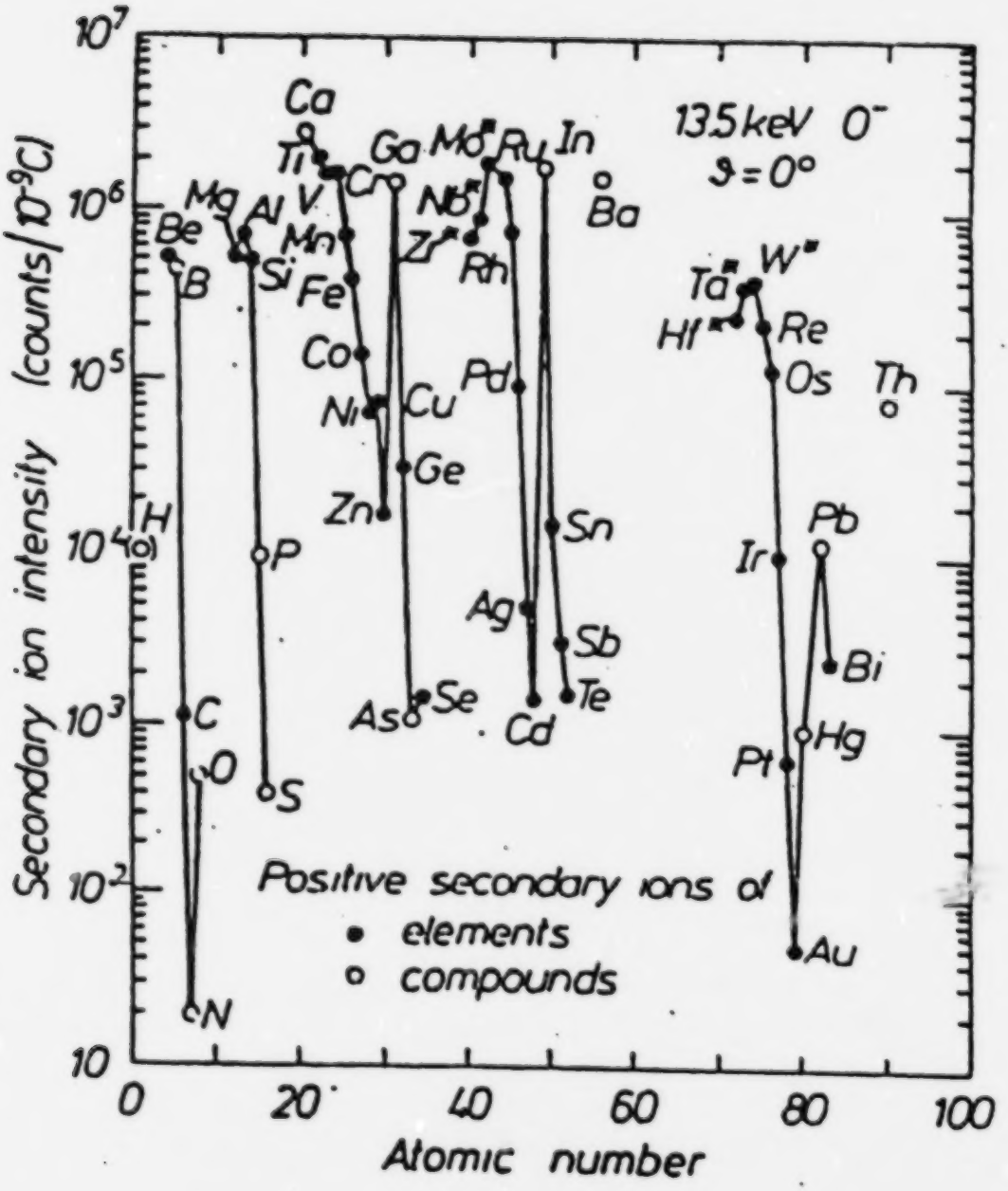

FIGURE 7: Relative positive secondary ion yield due to O^- bombardment vs atomic number of secondary ion (•) Pure element; (o) Compound (Storms et al., 1977)

5.2.4 Preparation of Standards

The standards for the calibration of the ion microprobe for ^{226}Ra in $BaSO_4$ and $PbSO_4$ were produced in the General Chemistry Laboratories of AECL in Chalk River. The ^{226}Ra that was used to prepare the standards was taken from a National Bureau of Standards (NBS) barium chloride solution certified for radium (100.0 ppm ^{226}Ra). The procedure followed to remove the barium from the NBS standard solution, and the preparation and certification of the radium stock solution are discussed in detail in Appendix A3.

The $(Ba,Ra)SO_4$ and $(Pb,Ra)SO_4$ standards were prepared by mixing the appropriate weighed quantity of the ^{226}Ra stock solution with the correct amount of a standard (1000 g/ml) barium and lead stock solution and co-precipitating the sulphates by addition of sulphuric acid. The weight of the ^{226}Ra solution was selected so as to yield 20 mg of a particular standard. Four standards of radium in $BaSO_4$ were prepared with nominal concentrations 5, 50, 100 and 250 ppm Ra. In the case of radium in $PbSO_4$ the nominal concentrations of the standards were 1, 5, 50 and 250 ppm.

The radium concentration in the prepared $BaSO_4$ and $PbSO_4$ standards was measured by γ-spectrometry of the precipitate (Table 5). In addition, analysis of the filtrates by α-spectrometry for radium and by atomic absorption for barium and lead verified that in all cases 99.9% of the barium, lead and radium had been precipitated from the solution (Appendix A3).

Elongate single or whisker-like aggregates of $(Ba,Ra)SO_4$ and $(Pb,Ra)SO_4$ crystals were formed ranging in size from a few microns up to twenty microns. Even after extended (1 week) contact with a saturated solution at $80^{\circ}C$ the crystals did not increase significantly in size.

Table 5. Radium Concentration in Barium and Lead Sulphate Standards

1. $BaSO_4$

Nominal Concentration	Ra Concentration in Precipitate (ppm)
5 ppm	5.3 ± 0.2
50 ppm	48 ± 2
100 ppm	97 ± 3
250 ppm	235 ± 7

2. $PbSO_4$

Nominal Concentration	Ra Concentration in Precipitate (ppm)
1 ppm	0.77 ± 0.03
5 ppm	6.9 ± 0.3
50 ppm	57 ± 2
250 ppm	279 ± 8

In order to obtain larger crystals the chemically reacted flux method was used (Patel and Koshy, 1968; Patel and Bhat, 1971) with some modifications. In this method the $(Ba,Ra)SO_4$ precipitates were filtered, the filter papers were transferred to platinum crucibles, ignited, Li_2SO_4 was added and the content heated to 800^oC to grow the $(Ba,Ra)SO_4$ crystals. The flux (Li_2SO_4) was dissolved in water and the $(Ba,Ra)SO_4$ crystals were washed and stored in polyethylene vials. The size of the $(Ba,Ra)SO_4$ crystals ranged from 100 to 500 μm.

The standards had to be homogeneous in terms of their radium content in order to be used for the calibration of the ion microprobe. Autoradiographs of $(Ba,Ra)SO_4$ crystals (Jucker and Treadwell, 1954) indicated that the distribution of radium in the $BaSO_4$ is uniform. SIMS analyses of individual crystals and of different areas in larger crystals of the $(Ba,Ra)SO_4$ standards produced by fusion confirmed the homogeneous distribution of radium (Appendix A4). However, this was not always the case with the $(Pb,Ra)SO_4$ crystals produced by fusion. Since the radium heterogeneity was believed to have been introduced during the Li_2SO_4-$(Pb,Ra)SO_4$ fusion (Appendix A3), a new series of $(Pb,Ra)SO_4$ standards was prepared by precipitation. In this second set of standards the radium was homogeneously distributed between the crystals (Appendix A4).

5.2.5 Development of the Technique

Oxygen minus O^- was selected as the primary beam for two reasons. First, radium belongs to group IIA of the alkaline earths and is immediately below barium in the periodic table, which is amongst the highest secondary ion yields with O^- (Figure 7). A periodicity, of the secondary ion yield and sputtering rate of the elements, as expressed in the periodic table, has been recognized (Storms et al., 1977). The high secondary ion yield of $^{226}Ra^+$ was verified in this study. In addition, practice has shown that O^- is preferable for analyzing insulating minerals because of minimum charging. Charging of the specimen can significantly alter the results of the ion microprobe when employing the external standardization method (Chryssoulis, 1986). No specimen charging (<5V) could be detected with primary currents up to 100nA.

Molecular interferences, which are common in SIMS have to be eliminated for quantitative ion microprobe analysis. Molecular interferences originate from molecular ions which have the same nominal mass and charge as the monoatomic ions of interest ($^{226}Ra^+$). In general, molecular ions have much narrower kinetic energy distributions compared to monoatomic ions, and therefore can be eliminated by applying the appropriate kinetic energy offset (Shimizu et al., 1978; Metson et al., 1983). Small differences in the mass can also be used to discriminate molecular from monoatomic ions (high mass resolution). Effectiveness in the elimination of the interfering molecular ion and loss in sensitivity are the criteria for selecting between the two methods.

In the case of barium sulphate the molecular ion interfering at 226 Daltons is $^{138}Ba^{88}Sr^+$. Strontium is a common trace element in barium sulphate and was present in both the Elliot Lake barite and the $(Ba,Ra)SO_4$ standards. A moderate high mass resolution ($M/\Delta M \sim 1{,}500$) successfully separated $^{138}Ba^{88}Sr^+$ from $^{226}Ra^+$ with limited loss in sensitivity (Figure 8).

In the case of the lead sulphate, energy offset gave better results in eliminating the molecular ion interfering at 226 Daltons ($^{208}Pb^{18}O^+$), when compared to high mass resolution (Figure 9). While ^{208}Pb is the most abundant lead isotope (52.3%), ^{18}O is rare (0.203%). The required energy offset was determined by measuring the intensity ratio $^{208}Pb^{16}O^+/(^{208}Pb^{18}O^+)$ as a function of increasing offset and comparing it against the $(^{208}Pb^{16}O^+/^{208}Pb^{18}O^+)$ ratio, which is equal to the $^{16}O^+/^{18}O^+$ ratio ($\sim$ 500). A -125V offset was sufficient in determining 1 ppm Ra in lead sulphate (Figure 10). A more severe offset may be required for Ra in the ppb range.

5.2.6 Calibration of the Ion Microprobe

The ion microprobe was calibrated for radium in a barium sulphate matrix using four synthetic radium doped barium sulphate standards with nominal concentrations 5, 50, 100 and 250 ppm Ra. From each standard at least ten grains were analyzed to determine the homogeneity of radium. The $BaSO_4$ grains were chosen so as to be both smaller and larger than the area of analysis (2800 μm) in order (i) to determine the effect of particle size upon the detectability of radium and (ii) evaluate interferences from the mounting epoxy. No interference or size related effects were seen. Results are given in Appendix A4. The intensity of $^{226}Ra^+$ was measured relative to that of $^{134}Ba^+$, typically for 400 to 800 seconds. The measured ion intensity ratios obtained from the doped barium sulphate crystals were plotted against the concentration of radium in parts per million (Figure 11). The radium concentration of the standards was established by by α counting of the solution before and after the $(Ba,Ra)SO_4$ precipitations and directly by γ counting of the precipitates. The resulting calibration curve is linear. The sensitivity of the analysis for radium in barium sulphate is better than 10 counts per second per part per million (cps/ppm).

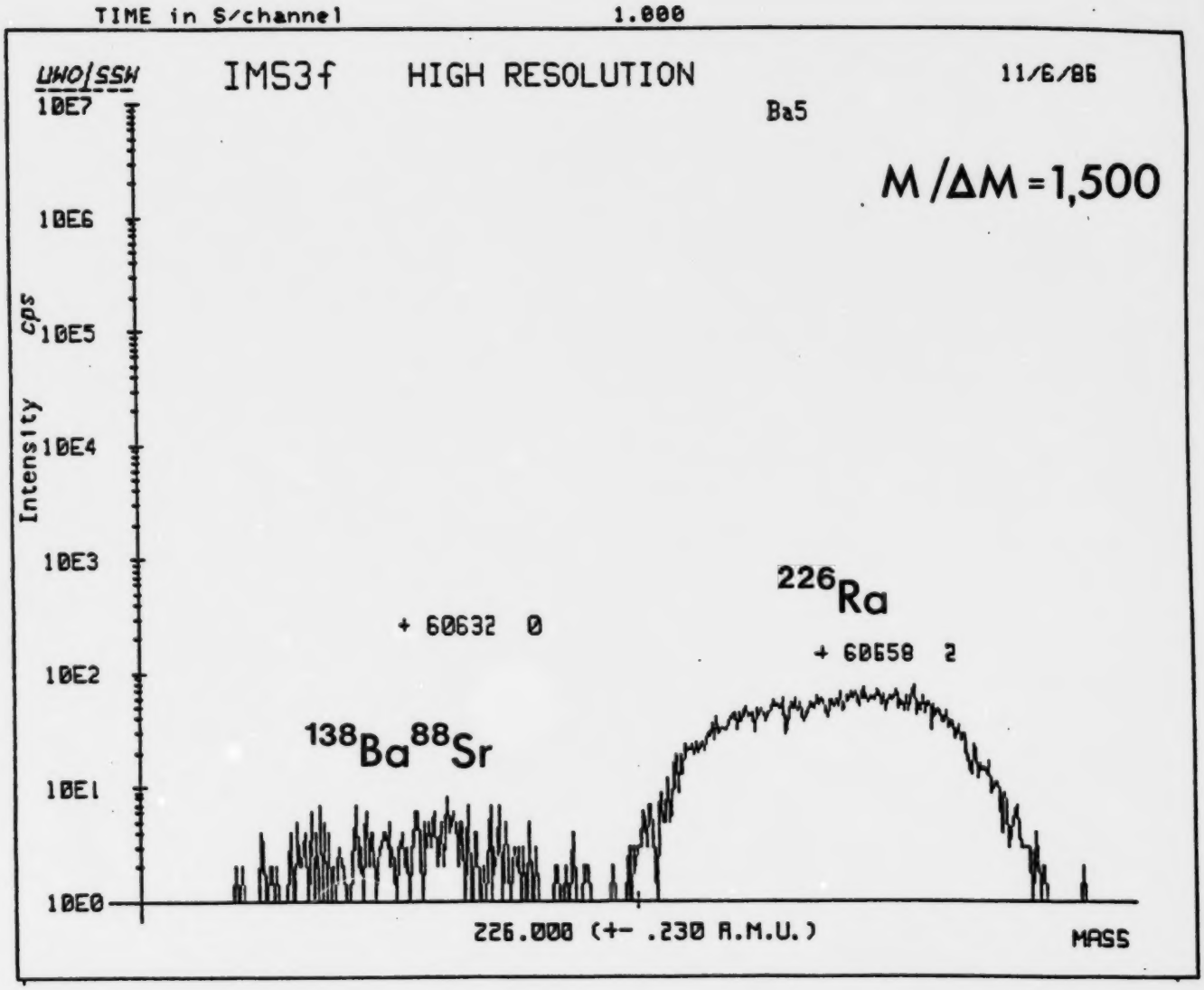

FIGURE 8: High mass resolution spectrum at 226 Daltons of a barium sulphate matrix ($^{138}Ba^{88}Sr^{+}$ = 225.81089, ^{226}Ra = 226.0254, M/ΔM = 1,054)

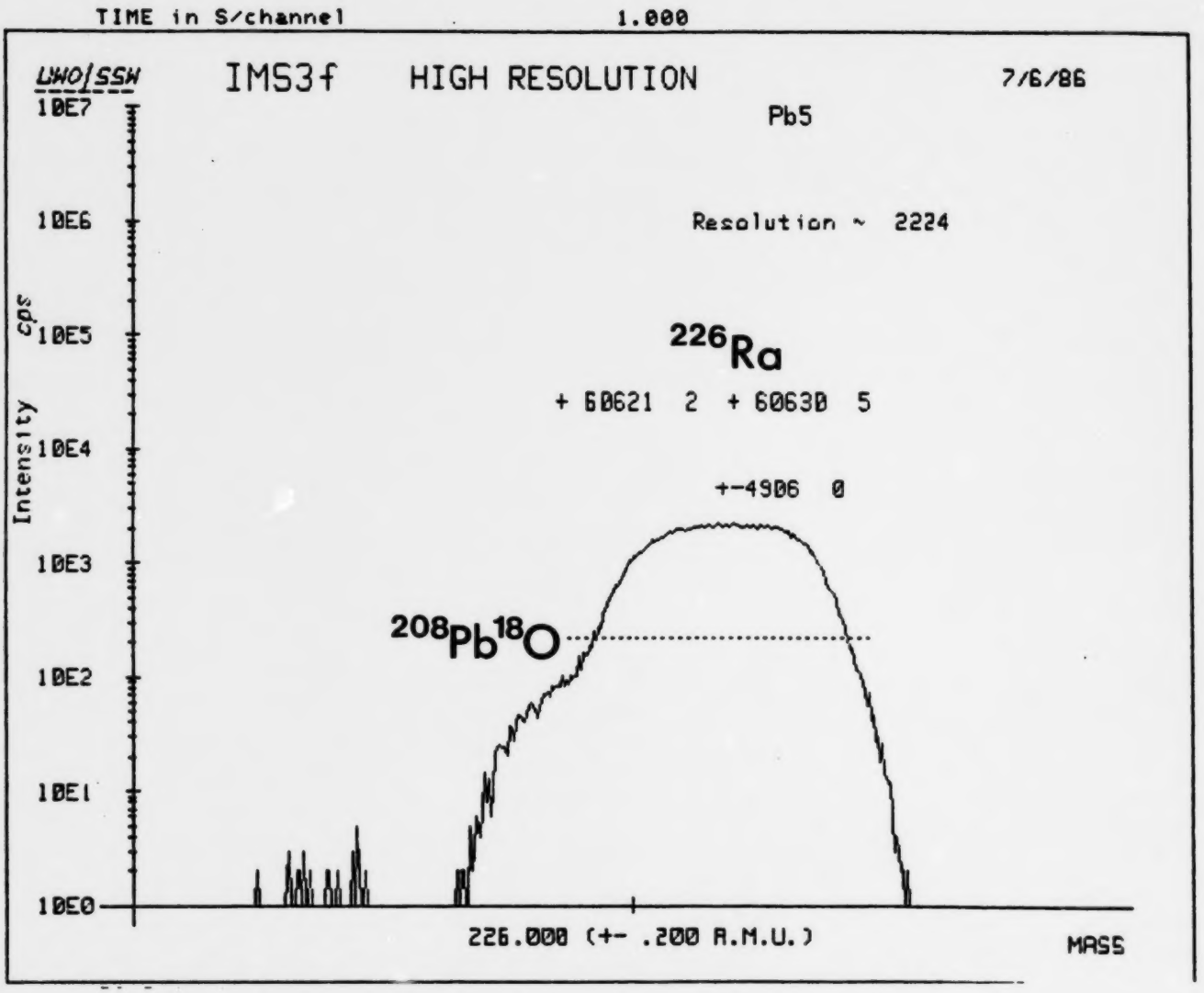

FIGURE 9: High mass resolution spectrum at 226 Daltons of a lead sulphate matrix ($^{208}Pb^{18}O^{+}$ = 225.97581, ^{226}Ra = 226.0254, M/ΔM = 4,558)

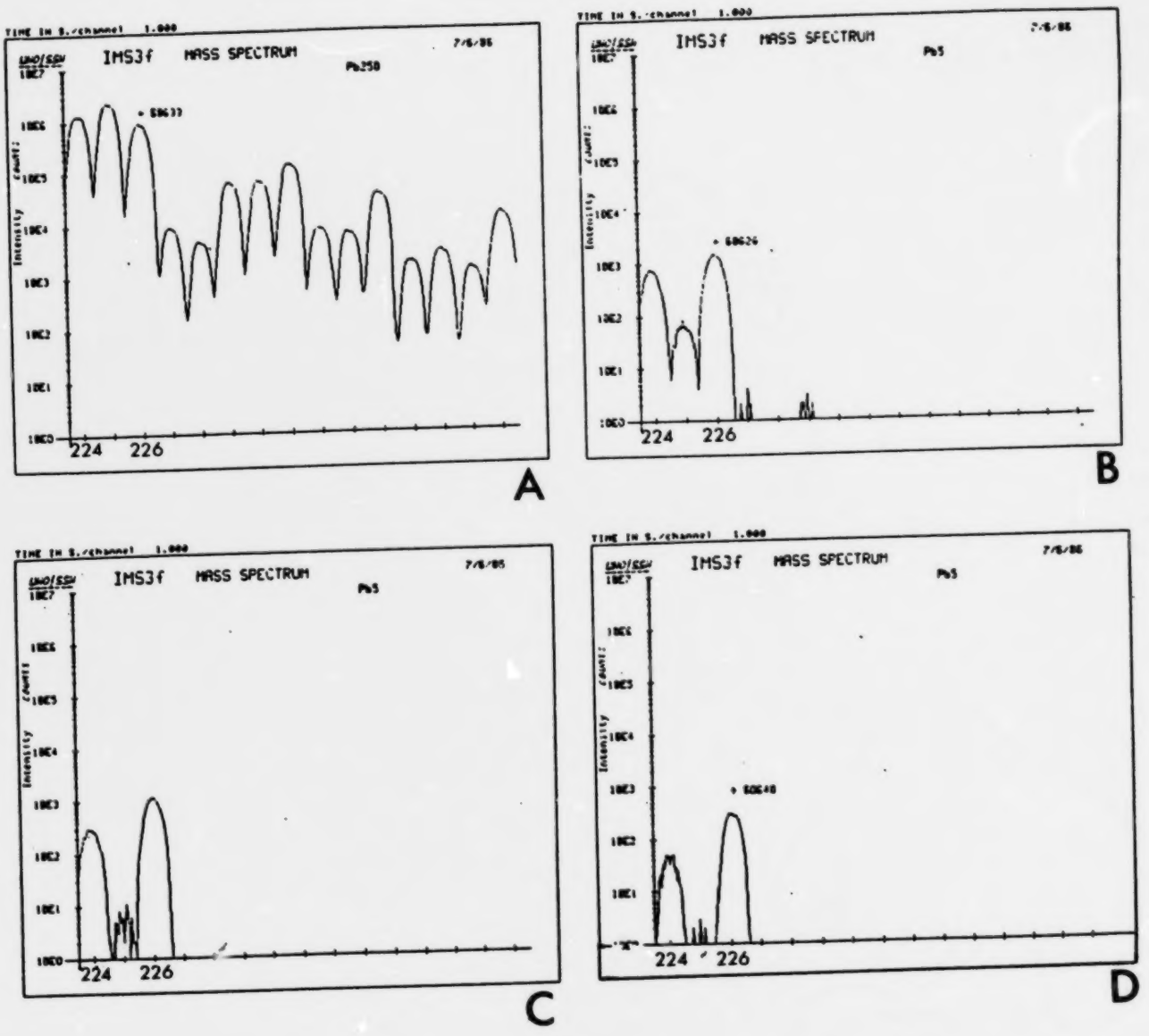

FIGURE 10: Mass spectra of synthetic $PbSO_4$ doped with radium, at various energy offsets. A. at zero offset molecular ions are not depressed, and the peak at 224 Daltons ($^{208}Pb^{16}O$) is more intense than the peak at 226 Daltons ($^{206}Pb^{18}O$, ^{226}Ra); B. with -125V offset most molecular ions are strongly depressed, and the intensity ratio of 224 over 226 reversed; C. with -175V offset the intensity ratio 224/226 is decreased further and; D. with -250V offset the 226 peak is exclusively due to radium (see text).

Figure 11: Calibration plot for the determination of radium in barium sulphate

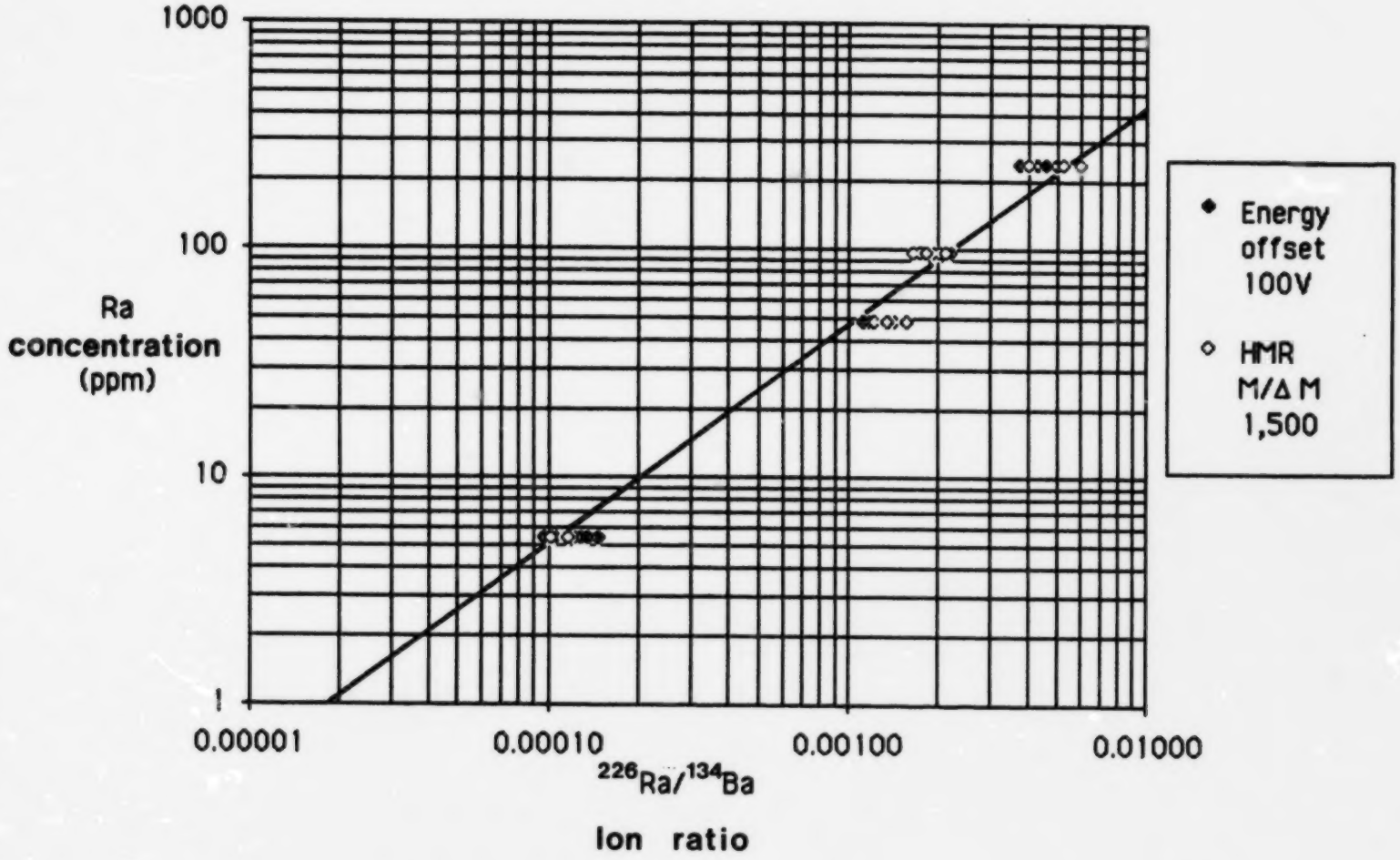

Four synthetic radium doped lead sulphate standards were prepared for the calibration of the ion microprobe, with nominal concentrations 1, 5, 50 and 250 ppm Ra. The exact concentration of radium in the standards was measured by α counting of the solution before and after the $(Pb,Ra)SO_4$ precipitation and directly by γ counting of the precipitate. The intensity of $^{226}Ra^+$ was measured relative to that of $^{206}Pb^+$, typically for 400 to 800 seconds. A calibration curve was constructed by plotting the measured ion intensity ratios obtained against the concentration of radium in parts per million (Figure 12). The sensitivity for radium analysis in lead sulphate is similar to that of radium in the barium sulphate.

Rather than blanks, a large barium sulphate (NMC64503) and lead sulphate crystal (NMC64570) obtained from the National Reference Collection (GSC) were analyzed with the ion microprobe for radium. Data on their radium content were not available during the preparation of this report.

The precision of the radium determinations is (15%) in the barium sulphate and (10%) in the lead sulphate. The precision was calculated by the Thompson and Howarth method (1976) from duplicate analyses of the same standard crystals in different runs. An evaluation of the accuracy of the method is not available.

The detection limit for the analysis of radium in barium and lead sulphate is a function of the intensity of the interfering molecular ion and the loss in sensitivity resulting from the required kinetic energy offset or high mass resolution to eliminate the interference. For a 60 µm diameter analysis area completely covered by the grain analyzed, a detection limit of 10-20 ppb is anticipated for strontium poor-barium sulphate. However, for the lead sulphate the detection limit is expected to be closer to 100 ppb of Ra since the interfering molecular ion is

Figure 12: Calibration plot for the determination of radium in lead sulphate

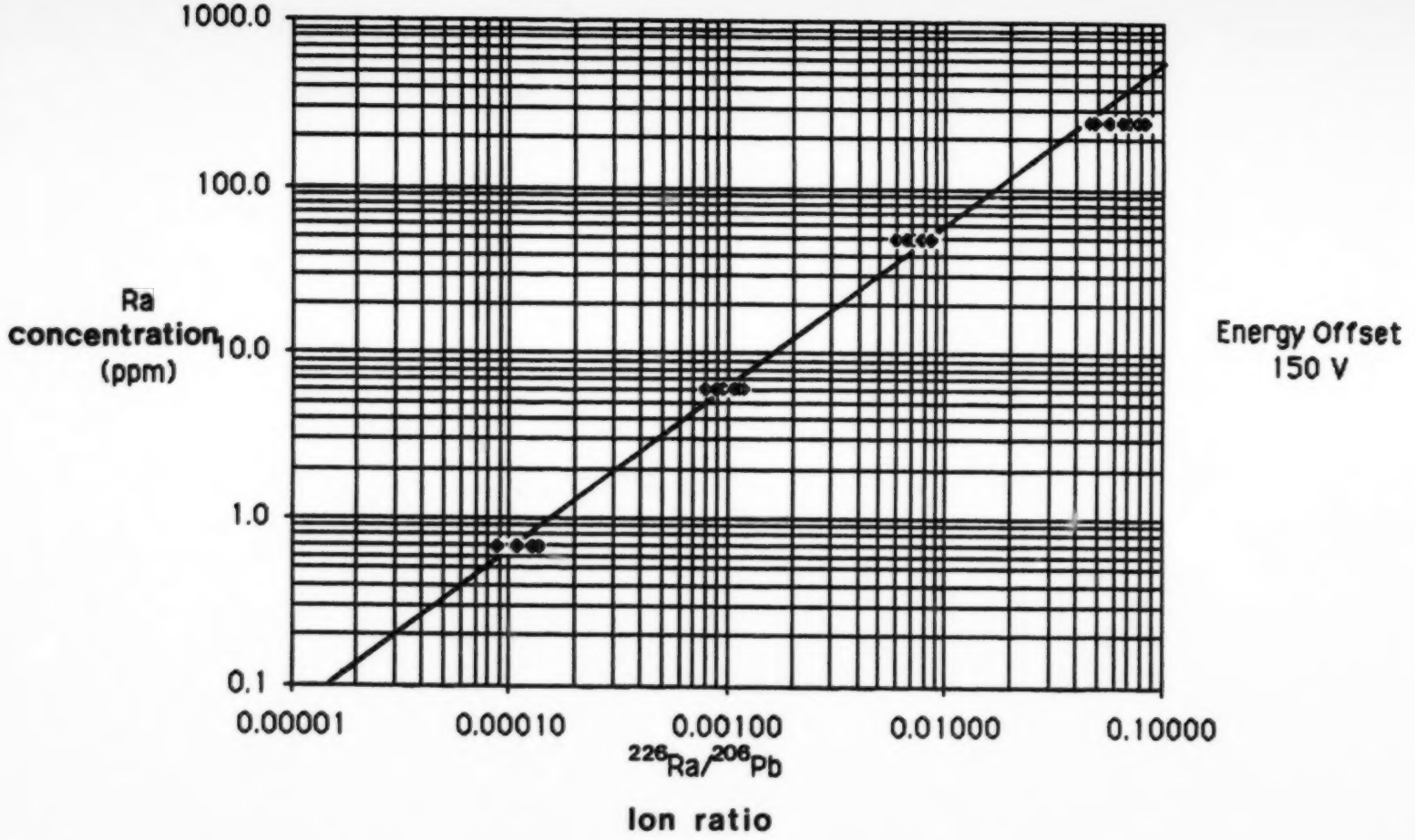

composed of major ions in the matrix. The detection limit increases as the size of the area of analysis decreases.

The ability to detect radium in small (1-10 μm) barium or lead sulphate grains is proportional to their radium concentration and inversely proportional to the size of the grains, for isolated grains embedded in the epoxy. Figure 13 depicts the decrease in the ^{226}Ra counts per 60 seconds with decreasing size of crystals containing 1 ppm Ra. The results depicted in Figure 13 were calculated from the analyses of the $PbSO_4$ crystals containing 50 ppm Ra. The size of the analyzed crystals was measured from BSE images (Appendix A2).

5.3 Determination of the Radium Concentration in the Elliot Lake Barite

The concentration of radium was determined in four large barite crystals (+60 μm) from the Elliot Lake ore (primary barium sulphate). A 60 μm in diameter area of analysis was used and was confined entirely within the grain analyzed. The counting time for radium had to be increased from 10 to 60 seconds because of the low count rate. All the determinations corresponded to concentrations below 100 ppb Ra. The lack of a standard in this range precludes the accurate determination of the radium content although it is probably above the detection limit of the method.

Secondary barium sulphate crystals which formed during the Pachuca leach were not found and therefore could not be analyzed with the ion microprobe. Their radium content is expected to be in the low ppm range based on available data from leaching tests (Steger and LeGeyt, 1986).

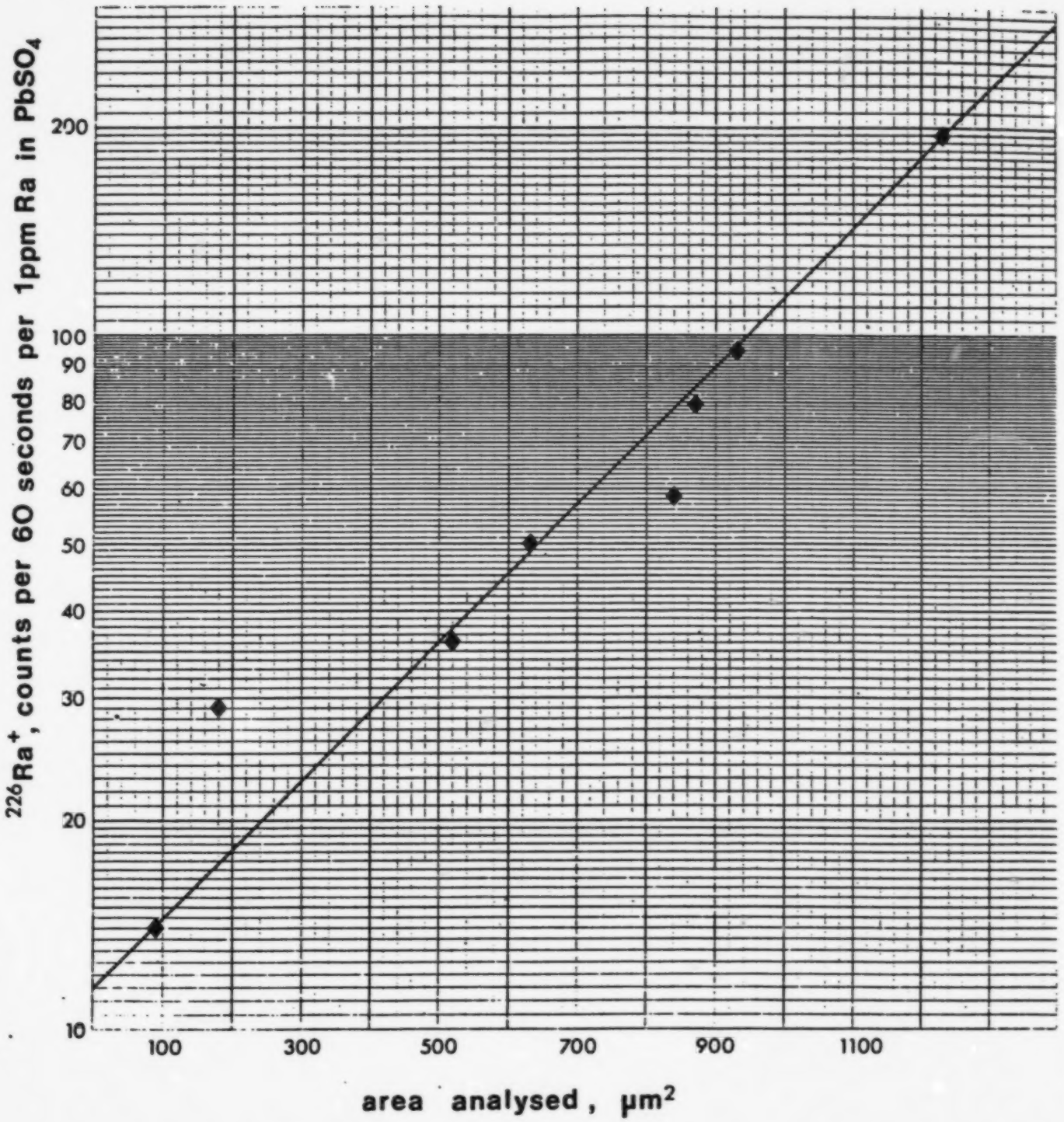

FIGURE 13: Sensitivity of the radium determination with the ion probe in $PbSO_4$ as a function of particle size ($PbSO_4$ particles mounted in epoxy).

6.0 DISCUSSION

6.1 Occurrence of Barium in Pachuca Solids

Extensive mineralogical examination of the pachuca solid samples obtained from Elliot Lake (Rio Algom) using a variety of microanalytical techniques revealed the presence of Barium in the following forms:

(i) Primary Barite
(ii) Barium in solid solution in potassium feldspar

Barium in the form of secondary barite formed during the pachuca leach process can be expected based on parallel studies (Snodgrass et al) but were not identified in this work.

Because sample preparation for SIMS analysis requires the selection of the larger grain sizes for examination, a program of size fractioning by wet screening and heavy media gravity separation was employed for this purpose. In addition, the polishing of epoxy mounted target grains results in the removal of all surface features to expose a flat section of the grain. It is most likely therefore, that these treatments resulted in the loss of most of the very small (1-2 μm), largely surface attached secondary precipitates of Barium.

6.2 Occurrence of Lead in Pachuca Solids

Lead in the pachuca solids was identified in the form of free galena grains and galena enclosed in pyrite. Lead may also be present in solid solution in the potassium feldspars (Wedepohl, 1969). Although the Elliot Lake feldspars were not analyzed for lead in solid-solution, sub-microscopic galena inclusions were identified.

Scanning electron microscopic examination of free galena grains revealed the presence of an oxidation rim which presumably

formed during the acid leaching process (Figure 5). In addition to the secondary lead sulphate forming in-situ around oxidizing galena grains, secondary precipitates of lead sulphate may also be expected to seed elsewhere, as in the case of secondary barium precipitates, particularly on the surface of potassium feldspar crystals. Furthermore, lead may co-precipitate with secondary barium sulphate. This has been recently confirmed by another study sponsored by the NUTP (Snodgrass et al).

6.3 Proposed Mechanism for the Dissolution and Precipitation of Radium, Barium and Lead in the Leach Process

During the Pachuca leach of uranium ores, radium is released into solution from the dissolving uranium minerals. At the same time in the highly acidic environment of the leach the potassium feldspar undergoes initial hydrolysis with K^+ being replaced by H^+ (Wollast, 1967). The Elliot Lake potassium feldspars are enriched in barium. The barium concentration of the feldspars range from below the detection limit of the electron microprobe in the EDS mode ($\sim$ 0.3 wt%) up to 6 wt%. Barium is also released during the initial hydrolysis. In the presence of an excess of sulphate ions the dissolved Ba^+ is precipitated as barium sulphate (secondary). Localized saturation of the process solution in barium sulphate is expected, in the vicinity of hydrolyzing barium-bearing feldspars resulting in the precipitation of barium sulphate preferentially on feldspar surfaces. Barite grains from the ore (primary barium sulphate) will dissolve until the solution becomes saturated with barium, when secondary barium sulphate enriched in radium will start coating the primary barite or seed elsewhere.

Although both primary barite and hydrolyzing barium-rich feldspar grains are sources of barium until the solution becomes saturated, once saturated, only the feldspar grains will continue to release barium into solution. The amount of barium in solutions at any time is determined by the rate of the initial hydrolysis of the feldspar grains and their barium content.

However, the amount of barium in solution is controlled by the degree of saturation in barium sulphate. Primary barite grains are not abundant and because of the common ion effect are expected to contribute little towards the dissolved barium.

Galena and probably the potassium feldspar (Wedepohl, 1969; Table 2, Pb assays of light fractions) are the main sources of lead released into solution during the Pachuca leach of the Elliot Lake uranium ore. The amount of lead released at any time from hydrolyzing potassium feldspars depends on their lead content and the rate at which the initial hydrolysis progresses. Therefore, once the primary barite and lead sulphate from the oxidized galena come into a dynamic equilibrium with the solution, the excessive barium and lead in solution originate from the feldspar crystals, their rate of release being the same and controlled by the rate of initial hydrolysis of feldspar.

The low radium concentration in the Pachuca leach solution precludes the formation of solid radium sulphate. Although radium sulphate is isomorphic to barium sulphate, available data indicate 'limited' isomorphism with lead sulphate (Vdovenko and Dubasov, 1975). Almost quantitative radium precipitation is reported with both sulphate salts. Therefore, prior to neutralization radium is removed from the solution by co-precipitation with secondary barium and lead sulphate salts.

Finally, the possibility of radium adsorbed on mineral grains is considered. At acid pH values radium is not likely to adsorb on mineral surfaces in significant amounts. However, at neutral pH values there is a distinct possibility of radium adsorption. Nikitin and Vdovenko (1936, 1937) determined the effect of pH and radium concentration on the amount of radium adsorbed on glass surfaces. The percent of adsorbed radium increased by one order of magnitude to 2.3% Ra, as the pH of the radium chloride solution containing 1×10^{-7} g/ml Ra was raised from 3.3 to 7.0. Similarly, the results indicate a sharp increase in the percent of

adsorbed radium at pH 7.0 from 0.55 to 7.07% Ra as the radium concentration changed from 2.6×10^{-6} to 4.4×10^{-9} g/ml Ra (Vdovenko and Dubasov, 1975).

Considering the rough surfaces of the mineral grains, the presence of sericite in the Elliot Lake ore (Kaiman, 1977) and the low radium concentration, it is expected that most of the radium, which is still in solution immediately prior to neutralization, will, upon the neutralization of the tailings, adsorb on the large mineral surface available, instead of co-precipitating with lead or barium sulphate. Murphy and Multamaki (1980) discussed the possibility of radium adsorbed on pyrite. Beard et al., (1979) determined the removal efficiencies of radium by phyllosilicate minerals. They range from 10% up to 78% in 10 minutes from solutions containing 525 pCi/l Ra.

In order to obtain a first estimate of the amount of radium adsorbed on the surface of mineral grains after neutralization, a mass balance for radium before the neutralization was attempted based on data tabulated in Table 6 (Barnes, 1986; per comm.). Assuming that all the radium in solution just before neutralization will be adsorbed, this amount is still insignificant (0.1 wt%).

6.4 Determination of Radium in Barium and Lead Sulphate by SIMS

The extraction rate for barium and lead and therefore radium is controlled by various factors including: rate of dissolution, solubility, grain size, age of precipitate, relative amounts of precipitates of different ages, all of which complicate the extraction of information from leaching tests. In-situ microanalytical techniques such as SIMS can be expected to provide a more direct means of identifying these host compounds of co-precipitated radium. While SIMS is a very sensitive technique it presently has a limited capability to analyze particles less than 10

μm in diameter because of the size of sampling area (625-3600 μm, Table 2) and the proportional increase in counting time associated with such small particles.

During the course of this study it became apparent that the secondary precipitates in the pachuca leach would predominate in the size range 1 to 10 μm. The precipitates induced during preparation of standards for the SIMS work were found to be in this size range, and this has also been confirmed after the completion of this study by the work of Snodgrass et al (1986) for samples from the Nordic tailings pond. Secondary barium and lead sulphates in this size range are believed to have been lost during sample preparation for this study. Finally, the radium content of the secondary precipitates are expected to be in the part per billion range (LeGeyt, 1986). Since the detection limit for radium in barium and lead sulphates, where the area of analysis is completely covered, are 20 and 100 ppb of radium respectively, it is clear that to analyze particles in the size range of interest here (1-10 μm) the radium concentration would need to be in the part per million range. These limitations are instrument specific. With the IMS-3F ion microprobe used in this study, the technique has been demonstrated to be quantitative, for radium in barium and lead sulphate at concentrations in the low ppm and possibly the ppb range provided that the area of analysis is completely covered.

The later generation IMS-4F, with liquid metal micron size primary beam and adjustable transfer optics may be capable of similar sensitivities for grains in the size range of the secondary sulphates (1-10 μm).

Table 6. Mass Balance of Radium Before Neutralization

		Solids	Liquid (out)
Volume %	:	70	30
Specific gravity (g/cc)	:	2.7	1.04 (72 g/l H_2SO_4)
Weight %	:	86	14
Ra concentration (pCi/g)	:	160	0.7-1
Radium balance	:	0.999	0.001

7.0 CONCLUSIONS

Elliot Lake Pachuca Solids

1. Barite was identified in the Elliot Lake ore.

2. The radium content of the barite present in the ore is less than 100 ppb Ra.

3. Barium-rich and barium-poor potassium feldspars were identified.

4. Although most of the barium in the Elliot Lake ore is probably in the potassium feldspars, that contributed by barite may be significant.

5. Both barium-bearing feldspars and barite are sources of soluble barium in the Pachuca leach.

6. Lead in the Elliot Lake ore is in the form of galena and probably in the potassium feldspars.

7. Free galena grains oxidize in the Pachuca leach and lead dissolves. Hydrolyzing potassium feldspar grains are another source of soluble lead.

8. (Secondary) barium and lead sulphate precipitates were not identified. It is suspected that they were lost during sample preparation.

Radium Doped Barium and Lead Sulphate Standards:

9. Fine grained (1-10 μm) precipitates of barium and lead sulphate salts doped with radium were prepared from NBS standard solution (100 μg/ml Ra). Prolonged crystallization failed to increase the grain size.

10. Coarse barium sulphate crystals (several millimeters) homogeneously doped with radium were prepared by fusion of $(Ba,Ra)SO_4$ precipitate with Li_2SO_4.

11. Coarse lead sulphate crystals (several millimeters) doped with radium were prepared by fusion of $(Pb,Ra)SO_4$ precipitate with Li_2SO_4. In all but one standard the radium was not homogeneously distributed.

Determination of Radium in Mineral Grains:

12. Reliable analysis for radium with the ion microprobe in barium and lead sulphate in the 1 to 250 ppm Ra concentration range was possible. Linear calibration curves were produced.

13. Not only is SIMS analysis suitable in the ppm range but this work has shown that it can be useful at ppb concentrations for both radium in barium sulphate and lead sulphate.

14. The ion microprobe (IMS-3F) enables the in-situ quantitative determination of radium in solids (50-60 μm diameter) when present in concentrations greater than a few tens of ppb Ra ($\simeq$ 1,000 Bq/g).

8.0 ACKNOWLEDGEMENTS

We acknowledge the contribution and assistance of Mr. Ted Barnes of Rio Algom Ltd., Elliot Lake, Ontario in providing the initial samples and for his guidance in our understanding of the process.

LIST OF REFERENCES

Beard, H.R., Nichols, 1.L. and Seidel, D.C., (1979); Absorption of radium and thorium from Wyoming and Utah uranium mill tailings solutions. Bureau of Mines Report, RI 8396, 15 p.

Chlopin, V.G. and Kuznetsova, V.I. (1939); Zhurnel Fizicheskoi Khimii 13, 1145, 1939

Chryssoulis, S.L., Chauvin, W.J. and Surges, L.J. (1986); Trace element analysis by secondary ion mass spectrometry with particular reference to silver in the Brunswick sphalerite. Submitted for publication. Canadian Metallurgical Quarterly.

Chryssoulis, S.L. (1986); Determination of silver in the Brunswick sphalerite, pyrite and chalcopyrite by SIMS. RPC unpublished report MDP/86/03.

Dana, J.D. and Dana, E.S. (1951); The system of mineralogy. John Wiley and Sons, New York, London 2, 411

Gaudin, A.M. (1957); Flotation. McGraw-Hill, New York

Jucher, H. and Treadwell, W.D. (1954); Helvetica Chimica Acta, 37, 2002

Kaiman, S. (1977); Mineralogical examination of old tailings from the Nordic Lake mine, Elliot Lake, Ontario. CANMET report ERP/MSL 77-190 (IR), 12 p.

Leta, D.P. and Morrison, G.H. (1980); Ion implantation for in-situ quantitative ion microprobe analysis. Analytical Chemistry, 52, 277-280.

McIntyre, N.S., Cabri, L.J., Chauvin, W.J. and Laflamme, J.H.G. (1984); Secondary ion mass spectrometric study of dissolved silver and indium in sulfide minerals. Scanning Electron Microscopy, 3, 1139-1146.

Merkulova, M.S. and Potapova, S.A. (1955); DAN SSSR, 103, 643.

Metson, J.B., Bancroft, G.M., McIntyre, N.S. and Chauvin, W.J. (1983); Suppression of molecular ions in the secondary ion mass spectra of minerals. Surface and Interface Analysis, 5, 181-185.

Murphy, K.L. and Multamaki, G.E., (1980); Placement of Radium/Barium sludges in tailings areas. Research Report AECB, INFO-0019, 54.

Patel, A.R. and Koshy, J. (1968); Growth of barium sulphate single crystals by chemically reacted flux method. Journal of Crystal Growth, 2, 128-130.

Patel, A.R. and Bhat, H.L. (1971); Growth of barite group crystals by the flux evaporation method. Journal of Crystal Growth, 11, 166-170.

Shimizu, N., Semet, M.P. and Allegre, C.J. (1978); Geochemical applications of quantitative ion microprobe analysis. Geochimica et Cosmochimica Acta, 42, 1321-1334.

Snodgrass, et al. (1986); Study of Radio barites in Uranium Mill Tailings. NUTP Report.

Steger, H.F. and LeGeyt, M. (1986); The dissolution of radium-226 in uranium mill tailings. Presentation at the CIC conference on June 3, 1986 in Saskatoon, Saskatchewan.

Storms, H.A., Brown, K.F. and Stein, J.D. (1977); Evaluation of cesium positive ion source for secondary ion mass spectrometry. Analytical Chemistry, 49, 2023.

Thompson, M. and Howarth, R.J. (1976); Duplicate analysis in geochemical practice in Part I, Theoretical approach and estimation of analytical reproducibility. Analysis, 101, 690-698.

Vdovenko, V.M. and Dubasov, Yu.V. (1975); Analytical chemistry of radium. John Wiley and Sons, New York-Toronto, 198 p.

Wedepohl, K.H. (1969); Handbook of Geochemistry, Volume 5, Springer-Verlag Berlin-Heidelberg.

Wollast, R. (1967); Kinetics of the alteration of k-feldspar in buffered solutions at low temperature. Geochimica et Cosmochimica Acta, 31, 635-648.

Zinner, E. (1980); Depth profiling by secondary ion mass spectrometry. Scanning, 3, 57-78.

APPENDIX A1

STATEMENT OF WORK

APPENDIX I

STATEMENT OF WORK

Study of Radium-226 Co-Precipitates in Uranium Mill Tailings by Secondary Ion-Mass Spectrometry

OBJECTIVES:

To study the barium and lead sulfate precipitates from uranium ore leaching by SIMS, secondary ion-mass spectrometry, to identify the one which radium-226 is the most likely to co-precipitate with for disposal as uranium mill tailings.

BACKGROUND:

The National Uranium Tailings Program is striving to develop mathematical models to predict future events pertaining to uranium tailings and to quantify and assign uncertainties to these predictions. To do so, data and information on the pathways of release of contaminants from the tailings in the long term are being obtained. Ra-226 is a major radionuclide contaminant in the tailings and its physical nature and ensuing reaction pathways must be well defined. Previous work has suggested that most of the radium-226 is co-precipitated with either barium or lead sulfate and its release depends on the dissolution of the host material, which is in turn determined by equilibrium with solution sulfate concentration. Further work is now underway but can at best lead only to an indirect identification of the most likely co-precipitate for radium-226. A study of the barium and lead sulfate precipitates in uranium leach pachuca solids by SIMS presents the possibility of identifying directly the sulfate with which radium-226 is most widely co-precipitated. SIMS is capable of analyzing samples with very small particle size for trace elements; the determination of radium-226 at a concentration as low as 6 ppm in individual particles of barium or lead sulfate is conceivable.

SCOPE OF WORK:

A Sole Source Proposal is being sought to apply the technique of secondary ion-mass spectrometry, SIMS, to a direct identification of the physical state of Ra-226 after uranium ore leaching with sulfuric acid in order to permit assigning probable dissolution mechanisms in the long term.

The proposed experimental application of SIMS should be designed to permit ultimately a comparison of the relative

tendency for the co-precipitation of radium-226 with either barium or lead sulfate. The proposal should take into account the procurement of pachuca leach solids.

APPENDIX A3

PREPARATION OF $(Ba,Ra)SO_4$ AND $(Pb,Ra)SO_4$ STANDARDS

Atomic Energy of Canada Limited
Research Company
Chalk River Nuclear Laboratories

L'Énergie Atomique du Canada, Limitée
Société de Recherche
Laboratoires Nucléaires de Chalk River

Chalk River, Ontario
Canada K0J 1J0
Telephone: 613-584-3311
Telex: 053-34555
Cable Address: "MOTA"
Telecopier: 613-589-2039
Word Processor Data Link: 613-589-2218

Reactor Materials Division
General Chemistry Branch

1986 August 15

Dr. S. Chrysoulis
RPC
P.O. Box 6000
Fredericton, N.B.
E3B 5H1

Preparation of $(Ba,Ra)SO_4$ and $(Pb,Ra)SO_4$ Standards

As requested we have prepared $BaSO_4$ crystals doped with ^{226}Ra at levels of 5, 50, 100 and 250 µg/g and $PbSO_4$ crystals doped with ^{226}Ra at levels of 1, 5, 50 and 250 µg/g. The procedures we have used to prepare the crystals are outlined below:

1. Preparation and Calibration of a Standard ^{226}Ra Stock Solution.

The ^{226}Ra that was used to prepare the crystals was taken from a National Bureau of Standards ^{226}Ra solution (see certificate enclosed) that contained 100.0 µg ^{226}Ra which was subsequently diluted by weight so as to contain 3.74×10^{-6} g ^{226}Ra per gram of solution. Unfortunately this ^{226}Ra standard solution contained a large but uncertain quantity of barium added by NBS as a "carrier" for radium. The first step in preparation of the crystals was the purification of the ^{226}Ra solution by separation of the radium from the barium on a cation exchange column using EDTA as eluent. Prior to cation exchange, a radioactive ^{133}Ba tracer was added to 4.9216 g of the NBS ^{226}Ra solution to enable us to follow the separation and determine the final purity of the ^{226}Ra solution by γ-spectrometry.

The barium-radium solution was loaded onto the cation exchange column and the barium was quantitatively eluted (>99.999%) before the pH of the eluent was raised to elute the ^{226}Ra. The ^{226}Ra fraction was diluted to a known weight in a 10.00 mL volumetric flask and the ^{226}Ra content was determined by evaporating and flaming a known weight of the ^{226}Ra solution on a platinum disk and measuring the absolute ^{226}Ra activity by α-spectrometry. The α-spectrometry system was calibrated under the identical geometry with an Amerstrom standard α-source (see certificate enclosed). The stock ^{226}Ra

...2

solution was determined to contain (6.48 ± 0.12) x 10^4 Bq ^{226}Ra per gram of solution. The overall uncertainty represents ±2S (95% confidence limits) calculated by summing in quadrature the reported uncertainties in the α-standard and the uncertainties due to counting statistics and solution weights. As an additional check, a mass balance for the ^{226}Ra was carried out by determining the ^{226}Ra content of the barium fraction and the column. The initial inventory of the NBS solution was 18.4 ± 0.1 µg ^{226}Ra while the ^{226}Ra measured in the solutions and column added up to 18.2 ± 0.4 µg which agree within the uncertainties.

2. Preparation of $(Ba,Ra)SO_4$ and $(Pb,Ra)SO_4$ Standards.

Initially you required 5, 50, 100 and 250 µg/g standards of radium in $BaSO_4$ and $PbSO_4$. An additional requirement was that the crystals had to be $\geq$100 µm along the shortest dimension to meet your beam scanning criteria. The most difficult task was meeting the size criteria. Both $BaSO_4$ and $PbSO_4$ crystals that were precipitated from solution only grew to a maximum length of 30 µm even after extended (1 week) contact with a saturated solution at 80°C. At your suggestion we attempted to grow the crystals at high temperature (850°C) using a low melting point alkali sulfate as the solvent. Lithium sulfate was selected and after experimenting with different solvent to solute ratios for different temperatures and times, a suitable combination was found. The next step was to prepare the $(Ba,Ra)SO_4$ and $(Pb,Ra)SO_4$ standards by co-precipitation followed by growth of the crystals in Li_2SO_4 at high temperature.

The $(Ba,Ra)SO_4$ and $(Pb,Ra)SO_4$ standards were prepared by mixing the appropriate weighed quantity of our ^{226}Ra stock solution with the correct amount of a standard (1000 µg/mL) barium and lead standard solution and co-precipitating the sulfates by addition of sulfuric acid. The weight of the ^{226}Ra solution was selected so as to yield 20 mg of a particular standard. An example of a calculation follows.

e.g. Preparation of ~5 ppm Ra in $BaSO_4$:

1) Weight of ^{226}Ra solution: 0.06094 g
2) Concentration of ^{226}Ra solution: 6.843x10^4 Bq/g
3) Concentration of Ba solution: 1000 µg/mL
4) Volume of Ba solution: 11.77 mL
5) Conversion factor for $Ba/BaSO_4$: 137.33/233.39
6) Conversion factor for Ra: 3.70x10^4 Bq/µg

...3

$$[Ra] = \frac{0.06094 \times 6.483 \times 10^4 \times 137.33}{3.70 \times 10^4 \times 1.00 \times 10^{-3} \times 11.77 \times 233.39} =$$

$= 5.34$ µg $^{226}Ra/g\ BaSO_4$.

The remaining $(Ba,Ra)SO_4$ standards were prepared in a similar manner.

The precipitation of the $(Ba,Ra)\ SO_4$ was carried out by first heating the mixed solution to 80°C, adding 2 mL H_2SO_4 and digesting at 80°C for 1-2 hr. The solution was allowed to cool and settle overnight and finally filtered through a 0.2 µm nitrocellulose filter. The filtrate was kept and analysed for barium by atomic absorption (AA) and for radium by α-spectrometry. In all cases >99.95% of the barium and radium had been co-precipitated from solution. The filter papers were then transferred to platinum crucibles, ignited, Li_2SO_4 added and the contents heated to 800°C to grow the $(Ba,Ra)SO_4$ crystals to the required size. The flux was dissolved in water and the $(Ba,Ra)SO_4$ crystals were washed and transferred to a polyethylene vial for shipment. The contents of the vials were assayed for ^{226}Ra by measuring the intensity of the 186 keV γ-ray of ^{226}Ra and no cross-contamination of the samples was detected.

Initially the $(Pb,Ra)SO_4$ standards were prepared according to the same procedure, however you indicated that upon analysis the crystals were not homogeneous within the same standard. The non-homogeneity may be due to differences in the melting points of the $PbSO_4$ and $RaSO_4$ or possibly due to differences in chemistry in the high temperature solution which might have caused some segregation of the radium and lead upon crystallization. As a result, we eliminated the last step involving growth of the crystals and prepared new $(Pb,Ra)SO_4$ standards from a stock solution of ^{226}Ra containing 7.769×10^3 Bq/g. The appropriate amount of ^{226}Ra solution was weighed out and mixed with the required amount of lead standard, the $(Pb,Ra)SO_4$ precipitated by addition of sulfuric acid, the precipitate was digested at 80°C, cooled and filtered through a 0.45 µm teflon filter. The filtrate was again checked for lead and radium and in all cases >99.94% of the radium and lead had been co-precipitated. The crystals were kept on the teflon filter for shipment and no cross-contamination was detected by γ-spectrometry.

The concentrations of the supplied standards are listed in TABLE 1 below.

...4

TABLE 1

Concentrations of $(Ba,Ra)SO_4$ and $(Pb,Ra)SO_4$ Standards

Standard		Concentration* (ppm)
$(Ba,Ra)SO_4$	5 ppm	5.3 ± 0.2
	50 ppm	48 ± 2
	100 ppm	97 ± 3
	250 ppm	235 ± 7
$(Pb,Ra)SO_4$	1 ppm	0.77 ± 0.03
	5 ppm	6.9 ± 0.3
	50 ppm	57 ± 2
	250 ppm	279 ± 8

* The concentration is reported as μg of radium per gram of the barium sulfate and lead sulfate. The uncertainties represent ±2S (95% confidence limits).

If you have any questions regarding the preparation of these standards, please do not hesitate to call me at 584-3311 local 2331.

KIB/ln

Enclosure

UNITED STATES DEPARTMENT OF COMMERCE
WASHINGTON

National Bureau of Standards

Certificate

FOR

RADIUM STANDARD

The sealed pyrex ampoule labelled "100.0 μg of Ra" contains, on this date

100.0×10^{-6} g of Radium

dissolved in a solution containing 4 percent of barium chloride ($BaCl_2 \cdot 2H_2O$) and 5 percent by weight of hydrogen chloride (HCl).

It is believed that the uncertainty in this value does not exceed 0.7 percent.

For the Director,
By

H. H. Seliger
Physicist
In Charge of Light Section

Order No. 3A-6-541
Test No. 125145-32
February 6, 1947

For a slight correction see
Journal of Research NBS Vol 62, 21 (1959)
W B Mann et al.
K. W. Geiger 21/6/83

(NO)

Description

Principal radionuclide: Americium-241, Curium-244, Plutonium-239

Product code: AMR.43

Source number: 9734RA

Measurement

Reference time: 1200 GMT on 8 November 1983

Rate of emergence of alpha particles from the front surface: 1.65×10^5 alpha particles per minute

Estimated disintegration rate of the active material: 3.24×10^5 disintegrations per minute

Measured ratios of the activities of Am-241/Cm-244/Pu-239: 1.000/1.053/1.336

Method of measurement:
The rate of emergence of alpha particles was measured in a proportional counter under conditions of 2-pi geometry.
The ratios of the activities of the radionuclides were measured using a gold surface barrier alpha spectrometer.

Accuracy

The overall uncertainty in the rate of emergence of alpha particles quoted above was: ± 2.0 %

The overall uncertainty in the ratio of the activities of any two radionuclides was: ± 2.0 %

The limits of uncertainty were taken as the arithmetic sum of the uncertainty due to random variations, calculated at the 99.7% confidence level, and the estimated systematic uncertainties in the measurement.

Physical Data

Radionuclide	Recommended half life	Important alpha particle energies MeV
Americium-241	433 years	5.442(12.5%), 5.484(85.2%)
Curium-244	17.8 years	5.763(23.6%), 5.806(76.4%)
Plutonium-239	24,100 years	5.103(11%), 5.142(15%), 5.155(73%)

Remarks

The ratio of the disintegration rate to the rate of emergence of alpha particles was estimated to be 1.96. This ratio includes the conversion from 2-pi to 4-pi geometry and the backscatter in the source. It assumes that there is no self-absorption in the active material.

The disintegration rate so derived does not include the disintegration rate of any traces of radioactive material that may be present in the source other than that on the front face. (Such activity is normally less than 5% of the total activity.)

A gold surface barrier alpha spectrometer was used to show that the measured alpha resolution (full width at half maximum height) was less than 20 keV.

Approved

Amersham

APPENDIX A4

ION PROBE MICROANALYSIS OF RADIUM IN SYNTHETIC BARIUM AND LEAD SULPHATES

Synthetic $(Ra,Ra)SO_4$ Standards

I.D.	Absolute Concentration (ppm)	Counts $^{226}Ra/^{134}Ba$	Mode O; Energy Offset H; HMR	
A	235.5	4.7622×10^{-3}	D	O
B	235.5	4.7035×10^{-3}	D	O
C	235.5	4.3045×10^{-3}	D	O
D	235.5	3.7841×10^{-3}	D	O
E	235.5	3.7767×10^{-3}	D	O
F	235.5	5.3574×10^{-3}	D	H
G	235.5	6.0768×10^{-3}		H
H	235.5	5.2735×10^{-3}		O
I	235.5	6.1420×10^{-3}		O
J	235.5	5.0406×10^{-3}		O
K	235.5	4.9968×10^{-3}		O
L	235.5	4.5888×10^{-3}		O
M	235.5	5.2519×10^{-3}		H
N	235.5	4.0341×10^{-3}		H
A	96.7	1.7834×10^{-3}	D	O
E	96.7	1.6484×10^{-3}	D	H
B	96.7	2.2084×10^{-3}	D	O
I	96.7	2.1264×10^{-3}	D	H
C	96.7	1.7177×10^{-3}		O
D	96.7	1.8006×10^{-3}	D	O
F	96.7	2.0282×10^{-3}	D	H
E	96.7	1.7516×10^{-3}		O
F	96.7	1.9132×10^{-3}		O
G	96.7	1.8254×10^{-3}		O
G	96.7	1.9471×10^{-3}		O
H	96.7	1.8161×10^{-3}		H
A	48.2	1.1664×10^{-3}	D	O
F	48.2	1.3786×10^{-3}	D	H
B	48.2	1.4201×10^{-3}	D	O
C	48.2	1.1283×10^{-3}		O
D	48.2	1.1930×10^{-3}		O
G	48.2	1.2317×10^{-3}		H
H	48.2	1.5707×10^{-3}		H
I	48.2	1.3611×10^{-3}	D	H
A	5.34	1.2337×10^{-4}		O
B	5.34	9.8772×10^{-5}		O
C	5.34	1.2595×10^{-4}		O
D	5.34	1.3078×10^{-4}		O
E	5.34	1.3518×10^{-4}	D	O
F	5.34	1.2883×10^{-4}	D	O
G	5.34	1.4765×10^{-4}		O
H	5.34	1.3573×10^{-5}	D	O
P	5.34	9.7625×10^{-4}		H
T	5.34	1.0652×10^{-4}	D	H
R	5.34	1.1631×10^{-4}		H
S	5.34	1.0273×10^{-4}		H

D: duplicate analysis

Synthetic $(Pb,Ra)SO_4$ Standards

I.D.	Absolute Concentration (ppm)	Counts $^{226}Ra/^{206}Pb$	Mode O; Energy Offset
B	279	7.5239×10^{-2}	O
C	279	7.6114×10^{-2}	O
D	279	7.5571×10^{-2}	O
F	279	5.8071×10^{-2}	O
G	279	4.7086×10^{-2}	O
H	279	4.8596×10^{-2}	O
I	279	7.1262×10^{-2}	O
J	279	7.7961×10^{-2}	O
I	279	8.2779×10^{-2}	O
J	279	6.5487×10^{-2}	O
16	57.3	5.9837×10^{-3}	O
15	57.3	7.1533×10^{-3}	O
14	57.3	7.7427×10^{-3}	O
7	57.3	8.4257×10^{-3}	O
6	57.3	7.7716×10^{-3}	O
13	57.3	8.0324×10^{-3}	O
2	57.3	8.7616×10^{-3}	O
4	57.3	7.8309×10^{-3}	O
5	57.3	8.7420×10^{-3}	O
11	57.3	6.7440×10^{-3}	O
0	6.95	1.1783×10^{-3}	O
1	6.95	9.6490×10^{-4}	O
2	6.95	7.9776×10^{-4}	O
3	6.95	8.8866×10^{-4}	O
6	6.95	1.1378×10^{-3}	O
7	6.95	1.0736×10^{-4}	O
0	0.77	1.1003×10^{-4}	O
0	0.77	1.3657×10^{-5}	O
4	0.77	8.8060×10^{-4}	O
1	0.77	1.0938×10^{-4}	O
4	0.77	1.2756×10^{-4}	O

Elliot Lake Barite

I.D.	Counts $^{226}Ra/^{134}Ba$	Mode
I-13	$3,2 \times 10^{-7}$	H
I-7	$5,2 \times 10^{-9}$	H
I-12	8.4×10^{-8}	H
I-14	8.06×10^{-8}	H

AUTHORIZATION

DEPARTMENT:

PROJECT TITLE:

PROJECT NUMBER: NUMBER PROPOSAL / REPORT

Prepared By:

Reviewed By:

Approved By:

Date: Aug. 19 1986

rpc RESEARCH AND PRODUCTIVITY COUNCIL
P.O. Box 6000, Fredericton, New Brunswick, Canada, E3B 5H1
Telephone (506) 452-8994
Telex 014-46115